

Preparation, Spectroscopic Characterization, X-ray Structure, and Theoretical Investigation of Hydride-, Dihydrogen-, and Acetone-OsTp Complexes: A Hydridotris(pyrazolyl)borate–Cyclopentadienyl Comparison

Ruth Castro-Rodrigo, Miguel A. Esteruelas,* Ana M. López,* Montserrat Oliván, and Enrique Oñate

Departamento de Química Inorgánica, Instituto de Ciencia de Materiales de Aragón, Universidad de Zaragoza-CSIC, 50009 Zaragoza, Spain

Received May 15, 2007

Complex $\text{OsH}_3\text{Cl}(\text{P}^i\text{Pr}_3)_2$ (**1**) reacts with KTp (Tp = hydridotris(pyrazolyl)borate) in tetrahydrofuran at room temperature to give $\text{OsH}_3(\kappa^2\text{-Tp})(\text{P}^i\text{Pr}_3)_2$ (**2**). In toluene at 80 °C, the κ^2 -Tp complex **2** is transformed to the κ^3 -Tp derivative $\text{OsH}_3\text{Tp}(\text{P}^i\text{Pr}_3)$ (**3**) in quantitative yield after 7 h. Protonation of **3** with HBF_4 affords the bis(dihydrogen) compound $[\text{OsTp}(\eta^2\text{-H}_2)_2(\text{P}^i\text{Pr}_3)]\text{BF}_4$ (**4**). In acetone complex **4** releases the coordinated hydrogen molecules in a sequential manner. At room temperature, the dihydrogen-solvate complex $[\text{OsTp}(\eta^2\text{-H}_2)(\kappa^1\text{-OCMe}_2)(\text{P}^i\text{Pr}_3)]\text{BF}_4$ (**5**) is formed, while at 56 °C the loss of both hydrogen molecules gives rise to the bis-solvento derivative $[\text{OsTp}(\kappa^1\text{-OCMe}_2)_2(\text{P}^i\text{Pr}_3)]\text{BF}_4$ (**6**). Complexes **2**–**6** have been characterized by X-ray diffraction analysis, and DFT calculations support their formulation. The structures of **3**–**5** have been compared with those of their Cp counterparts $\text{OsH}_3\text{Cp}(\text{P}^i\text{Pr}_3)$, $[\text{OsH}_2\text{-Cp}(\eta^2\text{-H}_2)(\text{P}^i\text{Pr}_3)]\text{BF}_4$, and $[\text{OsH}_2\text{Cp}(\kappa^1\text{-OCMe}_2)(\text{P}^i\text{Pr}_3)]\text{BF}_4$. The results show that the Tp ligand avoids piano stool geometries, while it enforces dispositions allowing N–Os–N angles close to 90° such as octahedron and pentagonal bipyramid.

Introduction

The hydrotis(pyrazolyl)borate (Tp) ligand¹ is frequently compared with the cyclopentadienyl (Cp) group due to the same number of electrons donated and the facial geometry adopted. However there are marked differences between them, in steric and electronic properties.² The cone angle of the Tp has been estimated to be as great as 180°, while that of Cp is calculated to be 100°. In addition, Tp is a weak-field ligand possessing relatively hard nitrogen σ donors, while the Cp group is relatively soft and capable of π donation. In contrast to Cp, the Tp ligand also strictly enforces an octahedral geometry around the metal center.

These differences are of great importance in hydride chemistry. The Tp ligand has a higher ability than Cp to stabilize nonclassical structures.³ For instance, while complexes $[\text{MCpH}_2\text{-LL}]^+$ (M = Fe, Ru, Os) can be dihydride or dihydrogen species,

the Tp counterparts are all dihydrogen derivatives.⁴ In contrast to the trihydride complexes $\text{RuCpH}_3(\text{PR}_3)$ and $\text{RuCp}^*\text{H}_3(\text{PR}_3)$ ($\text{Cp}^* = \text{C}_5\text{Me}_5$),⁵ the related compounds $\text{RuHTp}(\eta^2\text{-H}_2)(\text{PR}_3)$ have been described as hydride-dihydrogen species.⁶ The stabilization of bis(dihydrogen) complexes has been also achieved by using hydridotris(3-isopropyl-4-bromopyrazolyl)borate or hydridotris(3,5-dimethylpyrazolyl)borate (Tp') as a ligand in $\text{RuTp}'\text{H}(\eta^2\text{-H}_2)_2$.^{3a,7}

Osmium-hydride complexes have been shown to promote carbon–carbon and carbon–heteroatom coupling reactions.⁸ However, it is difficult to rationalize the processes because the products from the reactions of these compounds with unsaturated organic molecules depend on the interactions within the OsH_n units, and a further understanding of them is needed.⁹ We have recently prepared the complexes $\text{OsH}_3\text{Cp}(\text{P}^i\text{Pr}_3)$,¹⁰ $[\text{OsH}_2\text{Cp}(\eta^2\text{-H}_2)(\text{P}^i\text{Pr}_3)]\text{BF}_4$,¹¹ and $[\text{OsH}_2\text{Cp}(\kappa^1\text{-OCMe}_2)(\text{P}^i\text{Pr}_3)]\text{BF}_4$ ¹²

* Corresponding author. E-mail: maester@unizar.es; amlopez@unizar.es.

(1) (a) Trofimenko, S. *Chem. Rev.* **1993**, *93*, 943. (b) Trofimenko, S. *Polyhedron* **2004**, *23*, 197. (c) Pettinari, C.; Santini, C. In *Comprehensive Coordination Chemistry II*; McCleverty, J. A., Meyer, T. J., Eds.; Pergamon: Oxford, 2004; Vol. 1, pp 159–210. (d) Trofimenko, S. *J. Chem. Educ.* **2005**, *82*, 1715.

(2) (a) Kitajima, N.; Tolman, W. B. *Prog. Inorg. Chem.* **1995**, *43*, 419. (b) Gemel, C.; Trimmel, G.; Slugovc, C.; Kremel, S.; Mereiter, K.; Schmid, R.; Kirchner, K. *Organometallics* **1996**, *15*, 3998. (c) Tellers, D. M.; Bergman, R. G. *J. Am. Chem. Soc.* **2000**, *122*, 954. (d) Tellers, D. M.; Skoog, S. J.; Bergman, R. G.; Gunnoe, T. B.; Harman, W. D. *Organometallics* **2000**, *19*, 2428. (e) Rüba, E.; Simanko, W.; Mereiter, K.; Schmid, R.; Kirchner, K. *Inorg. Chem.* **2000**, *39*, 382. (f) Tellers, D. M.; Bergman, R. G. *Organometallics* **2001**, *20*, 4819. (g) Bengali, A. A.; Mezick, B. K.; Hart, M. N.; Fereshteh, S. *Organometallics* **2003**, *22*, 5436. (h) Bergman, R. G.; Cundari, T. R.; Gillespie, A. M.; Gunnoe, T. B.; Harman, W. D.; Klinckman, T. R.; Temple, M. D.; White, D. P. *Organometallics* **2003**, *22*, 2331. (i) Brunker, T. J.; Green, J. C.; O'Hare, D. *Inorg. Chem.* **2003**, *42*, 4366. (j) Beach, N. J.; Williamson, A. E.; Spivak, G. J. *J. Organomet. Chem.* **2005**, *690*, 4640.

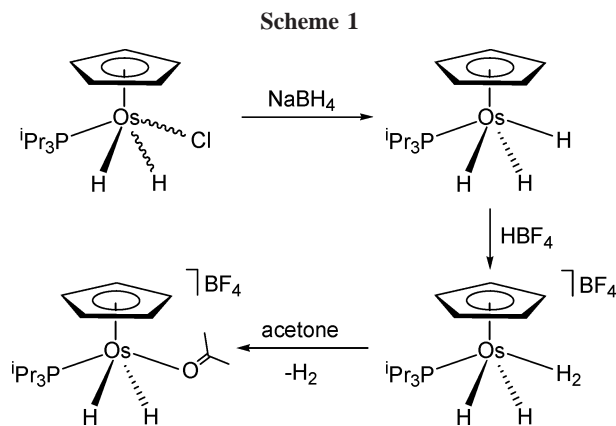
(3) See for example: (a) Moreno, B.; Sabo-Etienne, S.; Chaudret, B.; Rodríguez, A.; Jalon, F.; Trofimenko, S. *J. Am. Chem. Soc.* **1995**, *117*, 7441. (b) Chan, W.-C.; Lau, C.-P.; Chen, Y.-Z.; Fang, Y.-Q.; Ng, S.-M.; Jia, G. *Organometallics* **1997**, *16*, 34. (c) Oldham, W. J., Jr.; Hinkle, A. S.; Heinekey, D. M. *J. Am. Chem. Soc.* **1997**, *119*, 11028. (d) Gelabert, R.; Moreno, M.; Lluch, J. M.; Lledós, A. *Organometallics* **1997**, *16*, 3805. (e) Sabo-Etienne, S.; Chaudret, B. *Coord. Chem. Rev.* **1998**, *178–180*, 381. (f) Jiménez-Tenorio, M.; Palacios, M. D.; Puerta, M. C.; Valerga, P. *Organometallics* **2005**, *24*, 3088.

(4) Jia, C.; Lau, C.-P. *Coord. Chem. Rev.* **1999**, *190–192*, 83.

(5) (a) Suzuki, H.; Lee, D. H.; Oshima, N.; Moro-oka, Y. *Organometallics* **1987**, *6*, 1569. (b) Arliguie, T.; Border, C.; Chaudret, B.; Devillers, J.; Poilblanc, R. *Organometallics* **1989**, *8*, 1308. (c) Heinekey, D. M.; Payne, N. G.; Sofield, C. D. *Organometallics* **1990**, *9*, 2643.

(6) (a) Halcrow, M. A.; Chaudret, B.; Trofimenko, S. *J. Chem. Soc., Chem. Commun.* **1993**, 465. (b) Chen, Y.-Z.; Chan, W. C.; Lau, C. P.; Chu, H. S.; Lee, H. L.; Jia, G. *Organometallics* **1997**, *16*, 1241. (c) Jiménez Tenorio, M. A.; Jiménez Tenorio, M.; Puerta, M. C.; Valerga, P. *J. Chem. Soc., Dalton Trans.* **1998**, 3601.

(7) Moreno, B.; Sabo-Etienne, S.; Chaudret, B.; Rodríguez-Fernández, A.; Jalon, F.; Trofimenko, S. *J. Am. Chem. Soc.* **1994**, *116*, 2635.



(Scheme 1) and studied their reactions with ketones¹¹ and internal alkynes.¹² Now, our interest in rationalizing the reactivity of the OsH_n complexes toward unsaturated organic molecules prompts us to initiate a research program centered around the chemistry of the OsH_nTp(PⁱPr₃) counterparts.

Polyprazolyborate osmium complexes remain less explored than those of most d-block elements. In 1990 the synthesis of the dinuclear compound [TpOs(CO)₂]₂ was reported. Treatment of this species with Br₂ affords the mononuclear derivate OsTpBr(CO)₂.¹³ The mixed sandwich complex OsCpTp has been obtained by reaction of [OsCp(CH₃CN)₃]⁺ with KTp.¹⁴ Schrock has used the latter salt to prepare the alkyldiyne OsTp(≡C⁻Bu)(CH₂⁺Bu)(OTf)(py)₂ (OTf = trifluoromethanesulfonate),¹⁵ whereas Shapley has synthesized OsTp'(N)Ph₂ starting from [Os(N)Ph₂(py)₂]⁺BF₄⁻ and KTp'.¹⁶ The related nitride OsTp(N)Cl₂, reported by Mayer, has been the key to the development of a wide part of the OsTp chemistry.¹⁷ Recently Girolami has described the synthesis of OsHTp(COD) (COD = 1,5-cyclooctadiene), which has also shown to be useful to prepare an array of compounds.¹⁸ Tin trihydride OsTp(SnH₃)-{P(OR)₃}(PPh₃) (R = Me, Et) complexes have been prepared by reaction of the corresponding OsTpCl{P(OR)₃}(PPh₃) compounds with SnCl₂ and NaBH₄ in ethanol. Their reactions with

CO₂ lead to the formate derivatives OsTp{SnH[OC(H)=O]}-{P(OR)₃}(PPh₃).¹⁹

The OsTp-hydride complexes are particularly rare. They have been stabilized with phosphine co-ligands and formed via κ²-TpOs intermediates. For example, we have reported that the well-known complex OsHCl(CO)(PⁱPr₃)₂²⁰ reacts with NaTp to give OsH(κ²-Tp)(CO)(PⁱPr₃)₂, which loses a phosphine ligand when heated to reflux in toluene, generating OsHTp(CO)(Pⁱ-Pr₃).²¹ Similarly, OsPhCl(CO)(PPh₃)₂ reacts with KTp to give initially Os(κ²-Tp)Ph(CO)(PPh₃)₂, which by heating in toluene affords OsTpPh(CO)(PPh₃).²² Protonation of OsHTp(CO)(Pⁱ-Pr₃) with HBF₄ yields the dihydrogen [OsTp(η²-H₂)(CO)(Pⁱ-Pr₃)]BF₄.²¹ Jia²³ and Hill²⁴ have reported the synthesis of OsTpCl(PPh₃)₂ and its conversion to the monohydride OsHTp(PPh₃)₂. The protonation of this compound gives [OsTp(η²-H₂)(PPh₃)₂]⁺.²³

In this paper we report a new entry to the OsTp chemistry, which allows the preparation of OsH_nTp(PⁱPr₃) complexes, in particular the notable bis(dihydrogen) derivative [OsTp(η²-H₂)₂(PⁱPr₃)]BF₄, and the comparison with their Cp counterparts.

Results and Discussion

1. Introduction of the Tp Ligand: Preparation of OsH₂Tp(PⁱPr₃)

A method of general use to obtain complexes containing a cyclopentadienyl ligand in the Os–PⁱPr₃ chemistry involves the reaction between the dihydride-dichloro complex OsH₂-Cl₂(PⁱPr₃)₂²⁵ and a cyclopentadienyl derivative of an s- or p-block element.²⁶ However, the method employed to access OsCp derivatives is not useful to obtain an indenyl-osmium precursor. In contrast to the dihydride-dichloro, the related trihydride OsH₃Cl(PⁱPr₃)₂ (**1**) reacts with LiInd (Ind = indenyl) to afford the monohydride OsH(Ind)(PⁱPr₃)₂ in high yield.²⁷ This prompted us to explore the reaction of **1** with KTp, as a method to coordinate the Tp ligand to the osmium atom.

(8) (a) Esteruelas, M. A.; López, A. M. In *Recent Advances in Hydride Chemistry*; Peruzzini, M., Poli, R., Eds.; Elsevier: Amsterdam, 2001; Chapter 7, pp 189–248. (b) Castarlenas, R.; Esteruelas, M. A.; Oñate, E. *Organometallics* **2001**, *20*, 2294. (c) Esteruelas, M. A.; Herrero, J.; López, A. M.; Oliván, M. *Organometallics* **2001**, *20*, 3202. (d) Barrio, P.; Esteruelas, M. A.; Oñate, E. *Organometallics* **2004**, *23*, 1340. (e) Cobo, N.; Esteruelas, M. A.; González, F.; Herrero, J.; López, A. M.; Lucio, P.; Oliván, M. *J. Catal.* **2004**, *223*, 319. (f) Bolaño, T.; Castarlenas, R.; Esteruelas, M. A.; Oñate, E. *J. Am. Chem. Soc.* **2006**, *128*, 3965. (g) Esteruelas, M. A.; Fernández-Alvarez, F. J.; Oliván, M.; Oñate, E. *J. Am. Chem. Soc.* **2006**, *128*, 4596.

(9) (a) Esteruelas, M. A.; García-Yebra, C.; Oliván, M.; Oñate, E. *Organometallics* **2000**, *19*, 3260. (b) Barrio, P.; Esteruelas, M. A.; Oñate, E. *Organometallics* **2002**, *21*, 2491. (c) Barrio, P.; Esteruelas, M. A.; Oñate, E. *Organometallics* **2003**, *22*, 2472. (d) Esteruelas, M. A.; Lledós, A.; Oliván, M.; Oñate, E.; Tajada, M. A.; Ujaque, G. *Organometallics* **2003**, *22*, 3753. (e) Barrio, P.; Esteruelas, M. A.; Oñate, E. *J. Am. Chem. Soc.* **2004**, *126*, 1946. (f) Eguillor, B.; Esteruelas, M. A.; Oliván, M.; Oñate, E. *Organometallics* **2004**, *23*, 6015. (g) Eguillor, B.; Esteruelas, M. A.; Oliván, M.; Oñate, E. *Organometallics* **2005**, *24*, 1428.

(10) Baya, M.; Crochet, P.; Esteruelas, M. A.; Gutiérrez-Puebla, E.; Ruiz, N. *Organometallics* **1999**, *18*, 5034.

(11) Esteruelas, M. A.; Hernández, Y. A.; López, A. M.; Oliván, M.; Oñate, E. *Organometallics* **2005**, *24*, 5989.

(12) Esteruelas, M. A.; Hernández, Y. A.; López, A. M.; Oliván, M.; Oñate, E. *Organometallics* **2007**, *26*, 2193.

(13) De V. Steyn, M. M.; Singleton, E.; Hietkamp, S.; Liles, D. C. *J. Chem. Soc., Dalton Trans.* **1990**, 2991.

(14) Freedman, D. A.; Gill, T. P.; Blough, A. M.; Koefod, R. S.; Mann, K. R. *Inorg. Chem.* **1997**, *36*, 95.

(15) LaPointe, A. M.; Schrock, R. R.; Davis, W. M. *J. Am. Chem. Soc.* **1995**, *117*, 4802.

(16) Koch, J. L.; Shapley, P. A. *Organometallics* **1997**, *16*, 4071.

(17) (a) Crevier, T. J.; Lovell, S.; Mayer, J. M.; Rheingold, A. L.; Guzei, I. A. *J. Am. Chem. Soc.* **1998**, *120*, 6607. (b) Crevier, T. J.; Lovell, S.; Mayer, J. M. *Chem. Commun.* **1998**, 2371. (c) Crevier, T. J.; Bennett, B. K.; Soper, J. D.; Bowman, J. A.; Dehestani, A.; Hrovat, D. A.; Lovell, S.; Kaminsky, W.; Mayer, J. M. *J. Am. Chem. Soc.* **2001**, *123*, 1059. (d) Bennett, B. K.; Lovell, S.; Mayer, J. M. *J. Am. Chem. Soc.* **2001**, *123*, 4336. (e) Soper, J. D.; Bennett, B. K.; Lovell, S.; Mayer, J. M. *Inorg. Chem.* **2001**, *40*, 1888. (f) Bennett, B. K.; Pitteri, S. J.; Pilobello, L.; Lovell, S.; Kaminsky, W.; Mayer, J. M. *J. Chem. Soc., Dalton Trans.* **2001**, 3489. (g) Dehestani, A.; Kaminsky, W.; Mayer, J. M. *Inorg. Chem.* **2003**, *42*, 605. (h) Bennett, B. K.; Saganic, E.; Lovell, S.; Kaminsky, W.; Samuel, A.; Mayer, J. M. *Inorg. Chem.* **2003**, *42*, 4127. (i) Soper, J. D.; Mayer, J. M. *J. Am. Chem. Soc.* **2003**, *125*, 12217. (j) Soper, J. D.; Rhile, I. J.; DiPasquale, A. G.; Mayer, J. M. *Polyhedron* **2004**, *23*, 323. (k) Soper, J. D.; Saganic, E.; Weinberg, D.; Hrovat, D. A.; Benedict, J. B.; Kaminsky, W.; Mayer, J. M. *Inorg. Chem.* **2004**, *43*, 5804. (l) Wu, A.; Dehestani, A.; Saganic, E.; Crevier, T. J.; Kaminsky, W.; Cohen, D. E.; Mayer, J. M. *Inorg. Chim. Acta* **2006**, *359*, 2842.

(18) Dickinson, P. W.; Girolami, G. S. *Inorg. Chem.* **2006**, *45*, 5215. (19) Albertin, G.; Antoniutti, S.; Bacchi, A.; Bortoluzzi, M.; Pelizzi, G. Zanardo, G. *Organometallics* **2006**, *25*, 4235.

(20) (a) Esteruelas, M. A.; Werner, H. J. *Organomet. Chem.* **1986**, *303*, 221. (b) Esteruelas, M. A.; Oro, L. A. *Adv. Organomet. Chem.* **2001**, *47*, 1.

(21) Bohanna, C.; Esteruelas, M. A.; Gómez, A. V.; López, A. M.; Martínez, M.-P. *Organometallics* **1997**, *16*, 4464.

(22) Burns, I. D.; Hill, A. F.; White, A. J. P.; Williams, D. J.; Wilton-Ely, J. D. E. *T. Organometallics* **1998**, *17*, 1552.

(23) Ng, W. S.; Jia, G.; Hung, M. Y.; Lau, C. P.; Wong, K. Y.; Wen, L. *Organometallics* **1998**, *17*, 4556.

(24) Buriez, B.; Burns, I. D.; Hill, A. F.; White, A. J. P.; Williams, D. J.; Wilton-Ely, J. D. E. *T. Organometallics* **1999**, *18*, 1504.

(25) Aracama, M.; Esteruelas, M. A.; Lahoz, F. J.; López, J. A.; Meyer, U.; Oro, L. A.; Werner, H. *Inorg. Chem.* **1991**, *30*, 288.

(26) (a) Esteruelas, M. A.; López, A. M.; Ruiz, N.; Tolosa, J. I. *Organometallics* **1997**, *16*, 4657. (b) Esteruelas, M. A.; López, A. M.; Oñate, E.; Royo, E. *Organometallics* **2004**, *23*, 3021. (c) Esteruelas, M. A.; López, A. M.; Oñate, E.; Royo, E. *Organometallics* **2004**, *23*, 5633. (d) Esteruelas, M. A.; López, A. M. *Organometallics* **2005**, *24*, 3584.

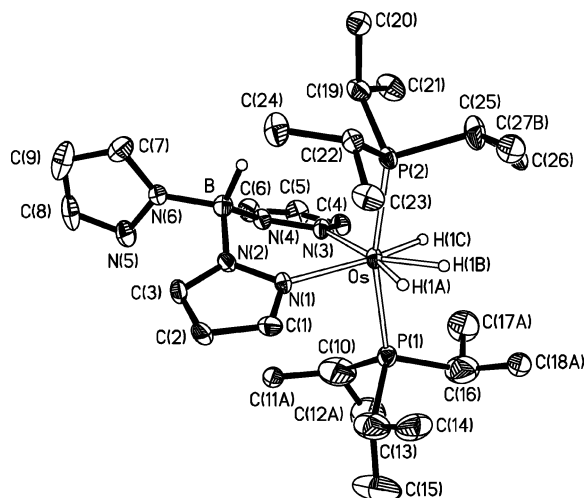


Figure 1. Molecular diagram of **2**. Selected bond lengths (Å) and angles (deg): Os–P(1) 2.3662(16), Os–P(2) 2.3471(16), Os–N(1) 2.197(4), Os–N(3) 2.194(4), Os–H(1A) 1.572(10), Os–H(1B) 1.582(10), Os–H(1C) 1.588(10); P(1)–Os–P(2) 165.75(5), P(1)–Os–N(1) 92.63(11), P(1)–Os–N(3) 92.60(12), P(2)–Os–N(1) 97.94(11), P(2)–Os–N(3) 97.61(12), N(1)–Os–N(3) 86.08(15).

Treatment of **1** with KTp in tetrahydrofuran at room temperature leads to the trihydride derivative $\text{OsH}_3(\kappa^2\text{-Tp})(\text{P}^i\text{Pr}_3)_2$ (**2**), which is isolated as a white solid in 85% yield. Its formation is the result of the substitution of the chloride ligand by two pyrazolyl groups of the Tp (eq 1).

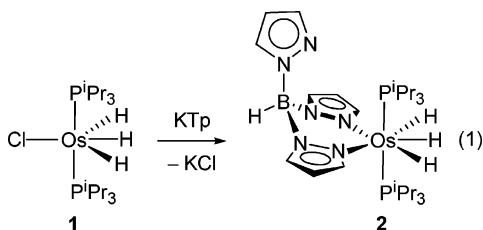


Figure 1 shows a molecular diagram of **2** obtained from X-ray diffraction data. The structure proves the bidentate coordination of the Tp ligand. The geometry around the osmium atom can be rationalized as a distorted pentagonal bipyramid with the phosphine ligands occupying axial positions (P(1)–Os–P(2) = 165.75(5)°). The metal coordination sphere is completed by the hydride ligands and the nitrogen atoms of the coordinated pyrazolyl groups of Tp, which acts with a bite angle of 86.08(15)°.

The hydride positions obtained from X-ray diffraction data are, in general, imprecise. However, DFT calculations have been shown to provide useful accurate data for the hydrogen positions in both classical polyhydride and dihydrogen complexes.²⁸ Thus, to know the positions of the hydrogen atoms of **2** bonded to the metal center, the B3LYP optimization of the structure of the model compound $\text{OsH}_3(\kappa^2\text{-Tp})(\text{PMe}_3)_2$ (**2t**) was performed (Figure 2). The OsH_3 unit adopts a disposition of local C_{2v} symmetry with N(1)–Os–H(1A) and N(3)–Os–H(1C) angles of 77.8° and 78.0°, respectively. The Os–H bond lengths for the terminal hydrogen atoms H(1A) and H(1C) are identical, 1.629 Å, whereas the central hydride H(1B) lies 1.605 Å from

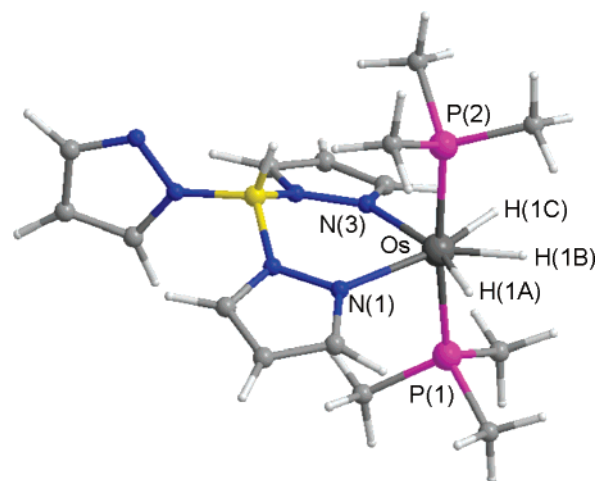


Figure 2. Optimized structure of **2t**. Selected bond lengths (Å) and angles (deg): Os–H(1A) 1.629, Os–H(1B) 1.605, Os–H(1C) 1.629, H(1A)⋯H(1B) 1.606, H(1B)⋯H(1C) 1.608; N(1)–Os–N(3) 85.0, N(1)–Os–H(1A) 77.8, N(3)–Os–H(1C) 78.0, H(1A)–Os–H(1B) 59.5, H(1B)–Os–H(1C) 59.6.

the metal. The separations between the latter atom and those of the corners are 1.606 (H(1A)–H(1B)) Å and 1.608 (H(1B)–H(1C)) Å.

In agreement with the structures shown in Figures 1 and 2, the $^{31}\text{P}\{^1\text{H}\}$ NMR spectrum of **2** in benzene- d_6 contains the expected AB spin system due to the inequivalent phosphine ligands. It appears at 22.9 ppm and is defined by $\Delta\nu = 412$ Hz and $J_{\text{A-B}} = 279$ Hz. The ^1H NMR spectrum is consistent with the $^{31}\text{P}\{^1\text{H}\}$ NMR spectrum and with the presence in the molecule of two types of pyrazolyl rings. Thus, it shows two sets of pyrazolyl resonances with a 1:2 intensity ratio, between 7.98 and 6.00 ppm. In the high-field region of the spectrum in toluene- d_8 , the inequivalent hydride ligands display only one signal, at –11.94 ppm, indicating that the hydrogen atoms bonded to osmium undergo a thermally activated site exchange process. The resonance appears as a triplet with a H–P coupling constant of 12.6 Hz. Lowering the sample temperature produces a broadening of the resonance. However, decoalescence is not observed down to 193 K. The T_1 values were determined at 300 MHz over the temperature range 273–213 K. A $T_{1(\text{min})}$ value of 70 ± 1 ms was obtained at 238 K.

The total relaxation rate for a H(n) hydride ligand ($R(n) = 1/T_{1(\text{min})(\text{H}(n))}$) is the addition of the relaxation rate due to the hydride dipole–dipole interactions (at 300 MHz $R_{\text{H-H}} = 129.18/r_{(\text{HH})}^6$) and that due to all other relaxation contributors (R^*).²⁹ Thus, one can obtain values of $T_{1(\text{min})}$ converted to the 300 MHz scale for each hydride ligand by using eqs 2–4, since R^* can be estimated to be 2.5 s^{-1} , the average value of those found in the trihydride–osmium compounds $[\text{OsH}_3(\text{diolofin})(\text{P}^i\text{Pr}_3)_2]\text{-BF}_4$.³⁰

$$R_{\text{H}(1\text{A})} = R^* + R_{\text{H}(1\text{A})-\text{H}(1\text{B})} + R_{\text{H}(1\text{A})-\text{H}(1\text{C})} \quad (2)$$

$$R_{\text{H}(1\text{B})} = R^* + R_{\text{H}(1\text{A})-\text{H}(1\text{B})} + R_{\text{H}(1\text{B})-\text{H}(1\text{C})} \quad (3)$$

$$R_{\text{H}(1\text{C})} = R^* + R_{\text{H}(1\text{A})-\text{H}(1\text{C})} + R_{\text{H}(1\text{B})-\text{H}(1\text{C})} \quad (4)$$

For exchange rates higher than 100 s^{-1} , as in this case at 238 K, the relaxation rate is the weighted average of the relaxation rate of each hydride (eq 5).³¹

(27) Esteruelas, M. A.; López, A. M.; Oñate, E.; Royo, E. *Organometallics* **2005**, *24*, 5780.

(28) Barrio, P.; Esteruelas, M. A.; Lledós, A.; Oñate, E.; Tomàs, J. *Organometallics* **2004**, *23*, 3008, and references therein.

(29) Jessop, P. G.; Morris, R. H. *Coord. Chem. Rev.* **1992**, *121*, 155.

(30) Castillo, A.; Esteruelas, M. A.; Oñate, E.; Ruiz, N. *J. Am. Chem. Soc.* **1997**, *119*, 9691.

$$R = (R_{H(1A)} + R_{H(1B)} + R_{H(1C)})/3 \quad (5)$$

Solving $R_{H(1A)}$, $R_{H(1B)}$, and $R_{H(1C)}$ yields an R value of 12.7 s^{-1} , which leads to a $T_{1(\text{min})}$ value of 79 ms, in good agreement with that determined by ^1H NMR spectroscopy.

Complex **2** is unstable in solution and slowly evolves into the κ^3 -Tp derivative $\text{OsH}_3\text{Tp}(\text{P}^i\text{Pr}_3)$ (**3**), as a result of the dissociation of one of the phosphine ligands of **2** and the coordination of the free pyrazolyl group to the metal center. In toluene at 80°C , the transformation is quantitative after 7 h. Complex **3** is isolated as a white solid in 70% yield (eq 6).

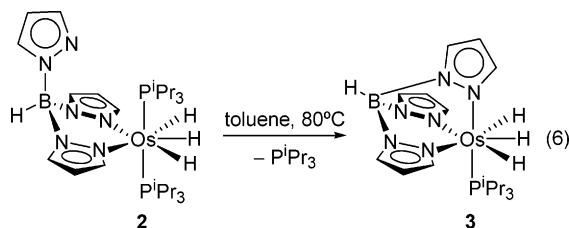


Figure 3 shows the structure of **3** obtained by X-ray diffraction analysis. The geometry around the osmium atom can be described as a distorted pentagonal bipyramid with the phosphine ligand and the N(5)-pyrazolyl group occupying axial positions ($\text{P}-\text{Os}-\text{N}(5) = 176.34(9)^\circ$). Like in **2**, the metal coordination sphere is completed by the hydride ligands and the nitrogen atoms N(1) and N(3) of the Tp ligand.

The B3LYP-optimized structure (Figure 4) of the model compound $\text{OsH}_3\text{Tp}(\text{PMe}_3)$ (**3t**) reveals that the OsH_3 unit adopts a disposition of local C_{2v} symmetry with both angles $\text{H}(1\text{A})-\text{Os}-\text{N}(1)$ and $\text{H}(1\text{C})-\text{Os}-\text{N}(3)$ of 79.3° . The osmium-hydride bond lengths of 1.627 ($\text{Os}-\text{H}(1\text{A})$), 1.601 ($\text{Os}-\text{H}(1\text{B})$), and 1.627 ($\text{Os}-\text{H}(1\text{C})$) Å, as well as the separations between the central hydride and those of the corners, of 1.613 ($\text{H}(1\text{A})-\text{H}(1\text{B})$) and 1.612 ($\text{H}(1\text{B})-\text{H}(1\text{C})$) Å, are in agreement with the respective parameters found in **2**.

In solution the axial and equatorial pyrazolyl groups exchange their positions. At room temperature the process proceeds at a rate sufficient to give rise to broad ill-defined resonances corresponding to only one type of pyrazolyl ring in the ^1H NMR spectrum. Lowering the sample temperature produces a broadening of the signals. Between 288 and 283 K two sets of pyrazolyl resonances with a 2:1 intensity ratio are clearly observed, in agreement with the structures shown in Figures 3 and 4. Line-shape analysis of the signals due to the central protons (Figure 5) allows the calculation of the rate constants for the position exchange process at different temperatures. The activation parameters obtained from the Eyring analysis are $\Delta H^\ddagger = 14.5 \pm 0.8 \text{ kcal}\cdot\text{mol}^{-1}$ and $\Delta S^\ddagger = 3.9 \pm 1.9 \text{ eu}$. The value of the activation entropy, close to zero, is consistent with an intramolecular process and indicates that the exchange takes place without the dissociation of any pyrazolyl group. Seven-coordinate Tp complexes are notorious for their fluxional behavior in solution,³² since none of the idealized geometries, capped prism, capped octahedron, or pentagonal bipyramid, nor any of the less symmetrical arrangements are characterized by a markedly lower total energy.³³

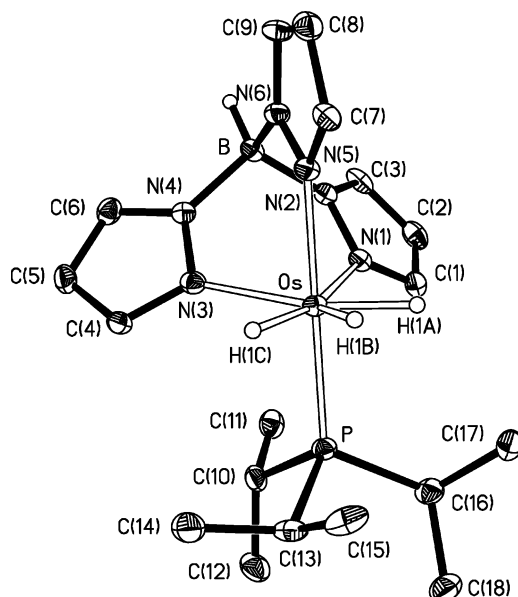


Figure 3. Molecular diagram of **3**. Selected bond lengths (Å) and angles (deg): Os–P 2.2803(11), Os–N(1) 2.182(3), Os–N(3) 2.163(3), Os–N(5) 2.137(3), Os–H(1A) 1.570(10), Os–H(1B) 1.570(10), Os–H(1C) 1.572(10); P–Os–N(1) 98.62(9), P–Os–N(3) 98.38(9), P–Os–N(5) 176.34(9), P–Os–H(1A) 86.9(12), P–Os–H(1B) 89.4(15), P–Os–H(1C) 85.9(14), N(1)–Os–N(3) 83.17(12), N(1)–Os–N(5) 84.71(12), N(3)–Os–N(5) 83.49(12), N(1)–Os–H(1A) 79.3(13), N(1)–Os–H(1B) 138.4(16), N(1)–Os–H(1C) 162.4(15), N(3)–Os–H(1A) 162.2(13), N(3)–Os–H(1B) 136.2(15), N(3)–Os–H(1C) 79.3(15), N(5)–Os–H(1A) 92.3(13), N(5)–Os–H(1B) 87.1(15), N(5)–Os–H(1C) 91.4(14), H(1A)–Os–H(1B) 60.4(17), H(1A)–Os–H(1C) 118.1(19), H(1B)–Os–H(1C) 58.2(18).

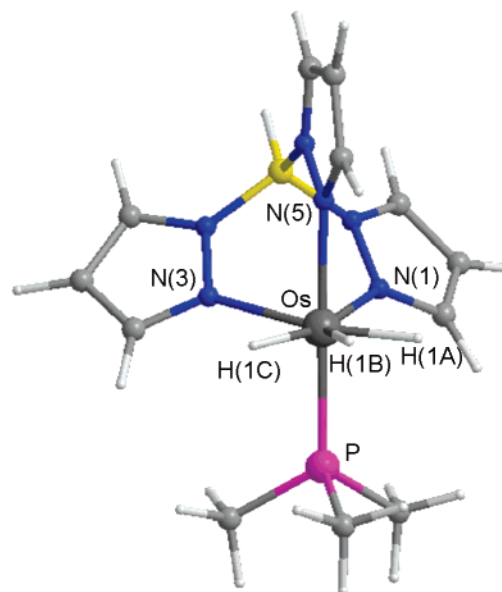


Figure 4. Optimized structure of **3t**. Selected bond lengths (Å) and angles (deg): Os–H(1A) 1.627, Os–H(1B) 1.601, Os–H(1C) 1.627, H(1A)⋯H(1B) 1.613, H(1B)⋯H(1C) 1.612; N(1)–Os–N(3) 82.1, N(1)–Os–H(1A) 79.3, N(3)–Os–H(1C) 79.3, H(1A)–Os–H(1B) 60.0, H(1B)–Os–H(1C) 59.9.

(31) Desrosiers, P. J.; Cai, L.; Lin, Z.; Richards, R.; Halpern, J. *J. Am. Chem. Soc.* **1991**, *113*, 4173.

(32) Curtis, M. D.; Shin, K.-B. *Inorg. Chem.* **1985**, *24*, 1213, and references therein.

(33) Alvarez, S.; Alemany, P.; Casanova, D.; Cirera, J.; Lluell, M.; Avnir, D. *Coord. Chem. Rev.* **2005**, *249*, 1693.

In contrast to **3**, the skeleton of **2** is rigid in solution. The behavior of this κ^2 -Tp complex agrees well with that previously observed for related $\text{OsH}_3(\text{YZ})(\text{P}^i\text{Pr}_3)_2$ and $\text{OsH}_2\text{X}(\text{YZ})(\text{P}^i\text{Pr}_3)_2$ (X = halogen, YZ = chelating ligand) species, where the presence of two bulky phosphine ligands appears to prevent

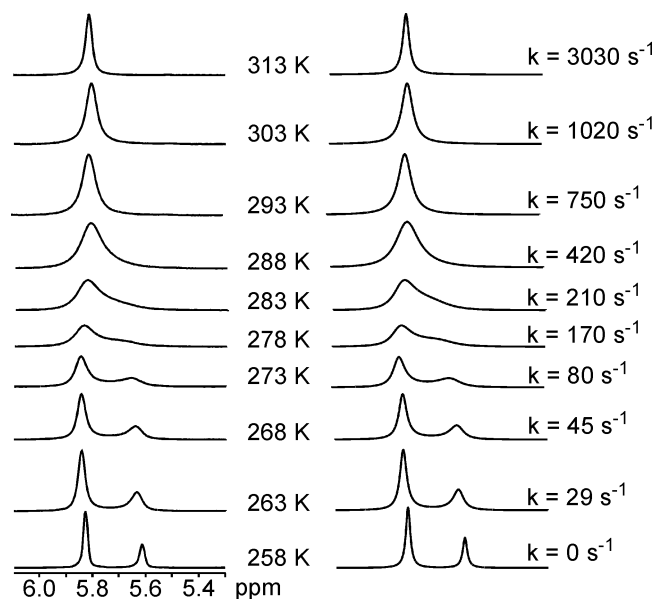


Figure 5. Variable-temperature $^1\text{H}\{^{31}\text{P}\}$ NMR spectra showing the H^4 -pz region of **3**: experimental in C_7D_8 (300 MHz, left) and calculated (right).

the necessary movements for the interconversion between polyhedra.^{30,34}

Like in **2**, the hydride ligands of **3** are involved in a thermally activated site exchange process, which has an activation barrier lower than that undergone by the pyrazolyl rings. Thus, at room temperature, the ^1H NMR spectrum in toluene- d_8 shows only a resonance for the inequivalent hydride ligands. It appears at -10.43 ppm as a doublet with a $\text{H}-\text{P}$ coupling constant of 15.0 Hz. At 238 K, in agreement with **2**, a $T_{1(\text{min})}$ value of 75 ms was obtained for this resonance in the 300 MHz scale. This value is similar to that calculated from the B3LYP-optimized structure of **3t** by means of eqs 2–5 (80 ms). In CDFCl_2 decoalescence occurs at 188 K. At 163 K, the $^1\text{H}\{^{31}\text{P}\}$ NMR spectrum shows an AB_2 spin system defined by $\delta_{\text{A}} -11.07$, $\delta_{\text{B}} -10.45$, and $J_{\text{AB}} = 420$ Hz.

Previous theoretical calculations on hydride site exchanges in related trihydride species suggest that the process takes place through dihydrogen transition states.^{34b,c,35} That for the exchange in **3t** has been located (**TS1**; Figure 6). It lies 11.2 kcal·mol $^{-1}$ above **3t** and has the coordinated $\text{H}(1\text{C})-\text{H}(1\text{B})$ molecule parallel disposed to the $\text{P}-\text{Os}-\text{N}(5)$ direction, with the atoms $\text{H}(1\text{C})$ and $\text{H}(1\text{B})$ separated by 0.925 Å.

The Cp counterpart $\text{OsH}_3\text{Cp}(\text{P}^i\text{Pr}_3)$ has been prepared by reaction of $\text{OsH}_2\text{CpCl}(\text{P}^i\text{Pr}_3)$ with NaBH_4 and methanol (Scheme 1).¹⁰ Recently, Girolami has similarly obtained the related $\text{OsH}_3(\eta^5\text{-C}_5\text{Me}_5)\text{L}$ ($\text{L} = \text{AsPh}_3, \text{PPh}_3, \text{PCy}_3, \text{PEt}_3$) compounds starting from the respective paramagnetic species $\text{Os}(\eta^5\text{-C}_5\text{Me}_5)\text{-Br}_2\text{L}$.³⁶ On the basis of the X-ray diffraction analysis of

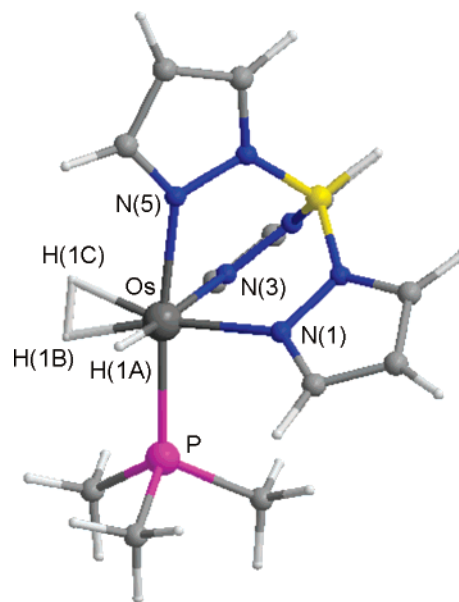


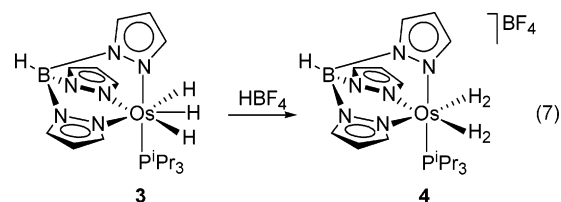
Figure 6. Optimized structure of **TS1**. Selected bond lengths (Å) and angles (deg): $\text{Os}-\text{H}(1\text{A})$ 1.635, $\text{Os}-\text{H}(1\text{B})$ 1.699, $\text{Os}-\text{H}(1\text{C})$ 1.694, $\text{H}(1\text{B})-\text{H}(1\text{C})$ 0.925; $\text{N}(1)-\text{Os}-\text{N}(3)$ 86.6, $\text{N}(1)-\text{Os}-\text{H}(1\text{A})$ 90.8, $\text{N}(3)-\text{Os}-\text{H}(1\text{B})$ 98.5, $\text{N}(3)-\text{Os}-\text{H}(1\text{C})$ 90.2, $\text{H}(1\text{A})-\text{Os}-\text{H}(1\text{B})$ 85.3, $\text{H}(1\text{A})-\text{Os}-\text{H}(1\text{C})$ 90.5, $\text{H}(1\text{B})-\text{Os}-\text{H}(1\text{C})$ 31.6.

$\text{OsH}_3(\eta^5\text{-C}_5\text{Me}_5)(\text{AsPh}_3)$ and $\text{OsH}_3(\eta^5\text{-C}_5\text{Me}_5)(\text{PPh}_3)$, the distribution of ligands around the metal center of these compounds has been described as a four-legged piano stool structure, which is now supported by the B3LYP-optimized structure of the model complex $\text{OsH}_3\text{Cp}(\text{PMe}_3)$ (**3t_{Cp}**, Figure 7a). The hydride separations are 1.791 ($\text{H}(1\text{A})-\text{H}(1\text{B})$), 1.792 ($\text{H}(1\text{B})-\text{H}(1\text{C})$), and 2.854 ($\text{H}(1\text{A})-\text{H}(1\text{C})$) Å.

In solution the hydride ligands of these compounds also undergo a thermally activated site exchange process. For $\text{OsH}_3\text{-Cp}(\text{P}^i\text{Pr}_3)$ the reported activated parameters are $\Delta H^\ddagger = 15.1 \pm 0.3$ kcal·mol $^{-1}$ and $\Delta S^\ddagger = 0.5 \pm 0.7$ eu.¹⁰ The located transition state for the hydride site exchange in **3t_{Cp}** is the three-legged piano stool **TS2** transition state shown in Figure 7b, which contains a coordinated $\text{H}(1\text{A})-\text{H}(1\text{B})$ molecule with a hydrogen-hydrogen separation of 0.981 Å, and lies 20.0 kcal·mol $^{-1}$ above **3t_{Cp}**.

The comparison of the facts observed for both Tp and Cp systems proves that Tp favors the hydride site activation process, in agreement with the higher tendency of Tp with regard to Cp to favor octahedral structures or related polyhedra with $\text{L}-\text{Os}-\text{L}$ angles close to 90° and therefore dihydrogen species.

2. Bis(dihydrogen) Complex $[\text{OsTp}(\eta^2\text{-H}_2)_2(\text{P}^i\text{Pr}_3)]\text{BF}_4$. The addition at room temperature of 1.2 equiv of $\text{HBF}_4 \cdot \text{Et}_2\text{O}$ to diethyl ether solutions of **3** gives rise to $[\text{OsTp}(\eta^2\text{-H}_2)_2(\text{P}^i\text{Pr}_3)]\text{BF}_4$ (**4**), as a consequence of the protonation of the starting compound. This bis(dihydrogen) derivative is isolated as a white solid in 91% yield, according to eq 7.



Complex **4** has also been characterized by X-ray diffraction analysis. The structure has two chemically equivalent but crystallographically independent molecules in the asymmetric

(34) (a) Esteruelas, M. A.; Lahoz, F. J.; López, A. M.; Oñate, E.; Oro, L. A.; Ruiz, N.; Sola, E.; Tolosa, J. I. *Inorg. Chem.* **1996**, *35*, 7811. (b) Barea, G.; Esteruelas, M. A.; Lledós, A.; López, A. M.; Oñate, E.; Tolosa, J. I. *Organometallics* **1998**, *17*, 4065. (c) Castillo, A.; Barea, G.; Esteruelas, M. A.; Lahoz, F. J.; Lledós, A.; Maseras, F.; Modrego, J.; Oñate, E.; Oro, L. A.; Ruiz, N.; Sola, E. *Inorg. Chem.* **1999**, *38*, 1814. (d) Castarlenas, R.; Esteruelas, M. A.; Gutierrez-Puebla, E.; Jean, Y.; Lledós, A.; Martín, M.; Tomàs, J. *Organometallics* **1999**, *18*, 4296.

(35) (a) Jarid, A.; Moreno, M.; Lledós, A.; Lluch, J. M.; Bertrán, J. J. *Am. Chem. Soc.* **1995**, *117*, 1069. (b) Demachy, I.; Esteruelas, M. A.; Jean, Y.; Lledós, A.; Maseras, F.; Oro, L. A.; Valero, C.; Volatron, F. J. *Am. Chem. Soc.* **1996**, *118*, 8388. (c) Camanyes, S.; Maseras, F.; Moreno, M.; Lledós, A.; Lluch, J. M.; Bertrán, J. J. *Am. Chem. Soc.* **1996**, *118*, 4617.

(36) Gross, C. L.; Girolami, G. S. *Organometallics* **2006**, *25*, 4792.

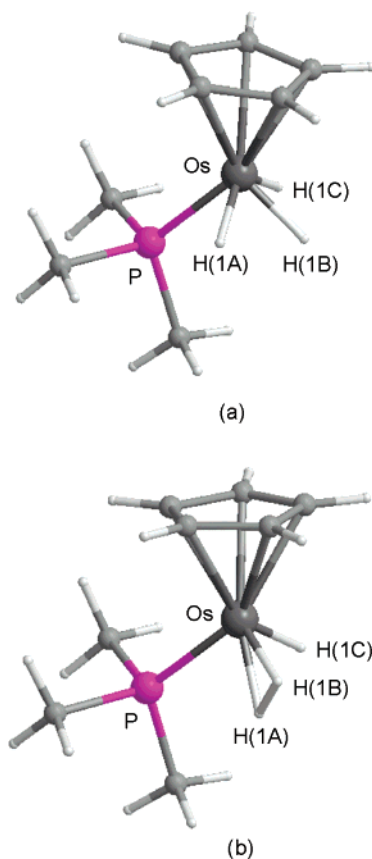


Figure 7. Optimized structures of $3t_{Cp}$ (a) and the transition state TS2 (b). (a) Selected bond lengths (Å) and angles (deg): Os–H(1A) 1.624, Os–H(1B) 1.611, Os–H(1C) 1.624, H(1A)–H(1B) 1.791, H(1B)–H(1C) 1.792; H(1A)–Os–H(1B) 67.3, H(1A)–Os–H(1C) 123.0, H(1B)–Os–H(1C) 67.3. (b) Selected bond lengths (Å) and angles (deg): Os–H(1A) 1.684, Os–H(1B) 1.669, Os–H(1C) 1.630, H(1A)–H(1B) 0.981; H(1A)–Os–H(1B) 34.0, H(1A)–Os–H(1C) 74.6, H(1B)–Os–H(1C) 91.6.

unit. Figure 8 shows a view of the cation of one of them. The geometry around the osmium atom can be described as a distorted octahedron with the terdentate ligand occupying *fac* positions and the phosphine ligand disposed *trans* to N(5) ($P(1)–Os(1)–N(5) = 176.5(2)^\circ$ in molecule a and $177.6(2)^\circ$ in molecule b).

The B3LYP-optimized structure (Figure 9) of the model cation $[OsTp(\eta^2-H_2)_2(PMe_3)]^+$ (**4t**) supports the bis(dihydrogen) nature of these species. The coordinated hydrogen molecules are symmetrically disposed to the sides of the plane containing the N(5)–Os–P and the N(5)–pyrazolyl ring, which is the symmetry plane of the cation, and are slightly inclined with regard to the N(5)–Os–P axis. The dihedral angles H–H–Os–N(5) and H–H–Os–P are 22.8° and 16.8° , respectively. The H–H bond length in both molecules is 0.906 Å.

The 1H NMR spectrum of **4** at room temperature in dichloromethane- d_2 shows a unique set of resonances for the inequivalent pyrazolyl groups, between 7.95 and 6.34 ppm. The equilibration in solution of the three pyrazolyl rings has been previously observed for other octahedral Tp transition metal complexes, and it has been attributed to the rotation of the N_3 face around the $B \cdots M$ axis.¹³ The process is thermally activated. Consistent with this, lowering the sample temperature leads to the broadening of the resonances. Between 223 and 213 K decoalescence occurs, and at temperatures lower than 203 K two sets of pyrazolyl signals in a 2:1 intensity ratio are observed, in agreement with the structures shown in Figures 8 and 9.

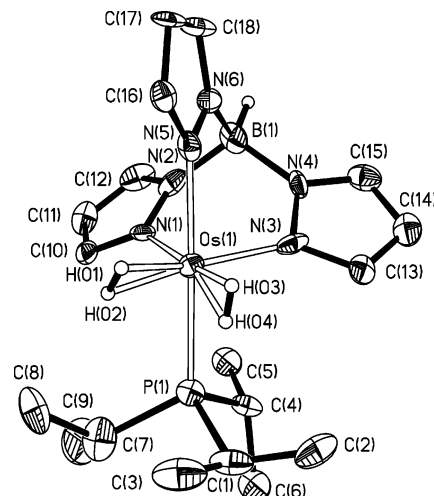


Figure 8. Molecular diagram of one of the two independent cations (cation a) of **4**. Selected bond lengths (Å) and angles (deg) for both cations (corresponding values for cation b are given in parentheses): Os(1)–P(1) 2.363(3) (2.382(3)), Os(1)–N(1) 2.095(8) (2.107(8)), Os(1)–N(3) 2.081(8) (2.098(7)), Os(1)–N(5) 2.124(7) (2.108(7)), Os(1)–H(01) 1.583(10) (1.581(10)), Os(1)–H(02) 1.579(10) (1.579(10)), Os(1)–H(03) 1.581(10) (1.582(11)), Os(1)–H(04) 1.582(10) (1.583(11)), H(01)–H(02) 0.84(1) (1.11(1)), H(03)–H(04) 0.65(1) (0.59(1)); P(1)–Os(1)–N(1) 94.9(2) (94.6(2)), P(1)–Os(1)–N(3) 95.0(2) (95.8(2)), P(1)–Os(1)–N(5) 176.5(2) (177.6(2)), N(1)–Os(1)–N(3) 88.0(3) (88.7(3)), N(1)–Os(1)–N(5) 81.7(3) (83.1(3)), N(3)–Os(1)–N(5) 84.5(3) (83.4(3)).

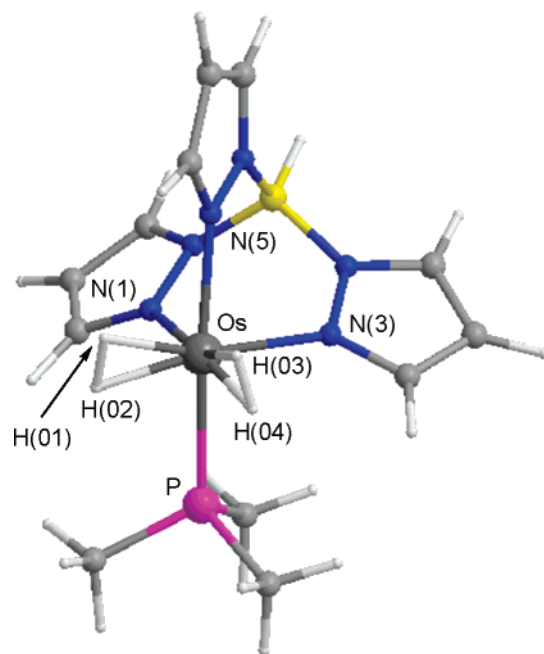


Figure 9. Optimized structure of the cation **4t**. Selected bond lengths (Å) and angles (deg): Os–H(01) 1.711, Os–H(02) 1.714, Os–H(03) 1.711, Os–H(04) 1.714, H(01)–H(02) 0.906, H(03)–H(04) 0.906; N(1)–Os–N(3) 88.7, N(1)–Os–H(01) 93.9, N(1)–Os–H(02) 85.8, N(3)–Os–H(03) 94.0, N(3)–Os–H(04) 85.8, H(01)–Os–H(02) 30.7, H(01)–Os–H(03) 78.5, H(01)–Os–H(04) 95.0, H(02)–Os–H(03) 95.0, H(02)–Os–H(04) 96.8, H(03)–Os–H(04) 30.7.

The activation parameters obtained for the fluxional process by means of the line-shape analysis of the signals due to the central hydrogen atoms of the pyrazolyl groups are $\Delta H^\ddagger = 9.3 \pm 0.3 \text{ kcal}\cdot\text{mol}^{-1}$ and $\Delta S^\ddagger = -5.1 \pm 1.9 \text{ eu}$.

In the high-field region of the ^1H NMR spectrum, the dihydrogen ligands display a doublet at -8.51 ppm with a H–P coupling constant of 7.5 Hz. At 300 MHz, the T_1 values of this resonance were determined over the temperature range 253–203 K. In accordance with the bis(dihydrogen) character of the complex, a $T_{1(\text{min})}$ value of 12 ± 1 ms was obtained at 208 K. Assuming fast spinning, this value corresponds to a hydrogen–hydrogen distance of 0.86 \AA ,^{29,37} which is only about 0.05 \AA shorter than that obtained by DFT calculations.

Few complexes containing two dihydrogen ligands are known. Ruthenium,^{3a,e,7,38} rhodium,³⁹ and iridium⁴⁰ derivatives have been characterized in solution by NMR spectroscopy or isolated as solids, whereas some chromium compounds have been observed in noble gas matrixes.⁴¹ For osmium, Caulton⁴² has reported that the protonation of $\text{OsH}_6(\text{P}^i\text{Pr}_3)_2$ with HBF_4 in acetonitrile initially affords $[\text{OsH}_3(\eta^2\text{-H}_2)_2(\text{P}^i\text{Pr}_3)_2]\text{BF}_4$, which undergoes loss of molecular hydrogen to give the trihydride derivative $[\text{OsH}_3(\text{CH}_3\text{CN})_2(\text{P}^i\text{Pr}_3)_2]\text{BF}_4$, and Gusev⁴³ has observed that in solution under hydrogen atmosphere $\text{OsH}_2\text{Cl}(\text{PCP})$ ($\text{PCP} = 2,6\text{-}(\text{CH}_2\text{P}^i\text{Bu}_2)_2\text{C}_6\text{H}_3$) forms $\text{OsH}_2\text{Cl}(\eta^2\text{-H}_2)(\text{PCP})$ via the bis(dihydrogen) intermediate $\text{OsCl}(\eta^2\text{-H}_2)_2(\text{PCP})$. In addition, it should be mentioned that, with the exception of the $\text{OsCl}(\eta^2\text{-H}_2)_2(\text{PCP})$ intermediate, the bis(dihydrogen) compounds of late transition metals contain also hydride ligands. In this context, it should be noted that complex **4** is a rare example of a stable bis(dihydrogen) derivative without hydride co-ligands.

The Cp counterpart of **4** is the dihydride-dihydrogen derivative $[\text{OsH}_2\text{Cp}(\eta^2\text{-H}_2)(\text{P}^i\text{Pr}_3)]\text{BF}_4$, which is obtained similarly to **4** by protonation with $\text{HBF}_4 \cdot \text{OEt}_2$ of the trihydride derivative $\text{OsH}_3\text{Cp}(\text{P}^i\text{Pr}_3)$ (Scheme 1), Cp counterpart of **3**. On the basis of a H–D coupling constant of 3.6 Hz, a separation between the hydrogen atoms of the coordinated hydrogen molecule of 1.1 \AA has been calculated.¹¹ This value agrees well with that found in the related pentamethylcyclopentadienyl complex $[\text{OsH}_2(\eta^5\text{-C}_5\text{Me}_5)(\eta^2\text{-H}_2)(\text{PPh}_3)]\text{BF}_4$ by spectroscopic methods (1.07 \AA)⁴⁴ and a single-crystal neutron diffraction study ($1.014\text{--}1.11 \text{ \AA}$).⁴⁵

In contrast to **4t**, two minima of similar energy ($\Delta E = 0.1 \text{ kcal}\cdot\text{mol}^{-1}$) have been found for the B3LYP-optimized structure of its Cp counterpart $[\text{OsH}_2\text{Cp}(\eta^2\text{-H}_2)(\text{PMe}_3)]^+$ (**4t_{Cp}**), **a** and **b** (Figure 10). Isomer **a** can be described as a *transoid*-dihydride

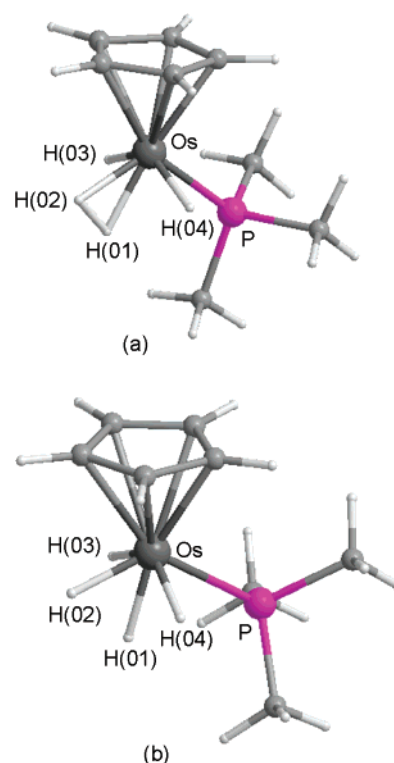


Figure 10. Optimized structures of the cation **4t_{Cp}**. (a) Selected bond lengths (Å) and angles (deg): Os–H(01) 1.698, Os–H(02) 1.685, Os–H(03) 1.632, Os–H(04) 1.634, H(01)–H(02) 0.955; H(01)–Os–H(02) 32.8. (b) Selected bond lengths (Å) and angles (deg): Os–H(01) 1.616, Os–H(02) 1.615, Os–H(03) 1.627, Os–H(04) 1.626, H(01)–H(02) 1.490; H(01)–Os–H(02) 54.9.

dihydrogen (H(01)–H(02) = 0.955 \AA) species, while isomer **b** can be rationalized as a *transoid*-dihydride elongated dihydrogen (H(01)–H(02) = 1.490 \AA) derivative. In a four-legged piano stool environment, the H_2 ligand of both structures lies in the plane containing the phosphorus and osmium atoms and the centroid of the Cp group.

The bonding interaction between the metal and the hydrogen molecule has been described in terms of donation from the filled σ -bonding orbital into an empty orbital of σ symmetry on the metal. This interaction is augmented by back-donation from filled metal orbitals of predominant d character to the σ^* orbital of the hydrogen molecule. Both interactions weaken and lengthen the hydrogen–hydrogen bond. In the limit of strong donation, bond cleavage to form two hydride ligands results.⁴⁶ As a consequence of this, the dihydrogen or dihydride character of a complex is sensitive to the nature of the co-ligands, which determines the electron density at the metal center. Comparison of the $\nu(\text{CO})$ IR data for $\text{MHTp}(\text{CO})(\text{P}^i\text{Pr}_3)$ and $\text{MHCp}(\text{CO})(\text{P}^i\text{Pr}_3)$ ($\text{M} = \text{Ru},^{21,47} \text{Os}^{21,48}$) shows that the electron-donating abilities of both metal fragments $\text{TpM}(\text{P}^i\text{Pr}_3)$ and $\text{CpM}(\text{P}^i\text{Pr}_3)$ are similar. In agreement with this, it has been observed that the separation between the hydrogen atoms of the coordinated hydrogen molecule in complexes $[\text{RuTp}(\eta^2\text{-H}_2)(\text{CO})(\text{P}^i\text{Pr}_3)]\text{BF}_4$ (0.95 \AA)²¹ and $[\text{RuCp}(\eta^2\text{-H}_2)(\text{CO})(\text{P}^i\text{Pr}_3)]\text{BF}_4$ (0.94 \AA)⁴⁷ is almost the same. So, the tendency of the Tp ligand to enforce an octahedral geometry is the leading force to the bis-

(37) Maltby, P. A.; Schlaf, M.; Steinbeck, M.; Lough, A. J.; Morris, R. H.; Klooster, W. T.; Koetzle, T. F.; Srivastava, R. C. *J. Am. Chem. Soc.* **1996**, *118*, 5396.

(38) (a) Arliguie, T.; Chaudret, B.; Morris, R. H.; Sella, A. *Inorg. Chem.* **1988**, *27*, 598. (b) Christ, M. L.; Sabo-Etienne, S.; Chaudret, B. *Organometallics* **1994**, *13*, 3800. (c) Rodriguez, V.; Sabo-Etienne, S.; Chaudret, B.; Thoburn, J.; Ulrich, S.; Limbach, H.-H.; Eckert, J.; Barthelat, J.-C.; Hussein, K.; Marsden, C. *J. Inorg. Chem.* **1998**, *37*, 3475. (d) Abdur-Rashid, K.; Gusev, D. G.; Lough, A. J.; Morris, R. H. *Organometallics* **2000**, *19*, 1652. (e) Borowski, A. F.; Donnadiou, B.; Daran, J.-C.; Sabo-Etienne, S.; Chaudret, B. *Chem. Commun.* **2000**, 543. (f) Giunta, D.; Hölscher, M.; Lehmann, C. W.; Mynott, R.; Wirtz, C.; Leitner, W. *Ad. Synth. Catal.* **2003**, *345*, 1139. (g) Grellier, M.; Vendier, L.; Chaudret, B.; Albinati, A.; Rizzato, S.; Mason, S.; Sabo-Etienne, S. *J. Am. Chem. Soc.* **2005**, *127*, 17592.

(39) Ingleson, M. J.; Brayshaw, S. K.; Mahon, M. F.; Ruggiero, G. D.; Weller, A. S. *Inorg. Chem.* **2005**, *44*, 3162.

(40) (a) Crabtree, R. H.; Lavin, M.; Bonneviot, L. *J. Am. Chem. Soc.* **1986**, *108*, 4032. (b) Cooper, A. C.; Eisenstein, O.; Caulton, K. G. *New J. Chem.* **1998**, 307.

(41) (a) Goff, S. E. J.; Nolan, T. F.; George, M. W.; Poliakoff, M. *Organometallics* **1998**, *17*, 2730. (b) Wang, X.; Andrews, L. *J. Phys. Chem. A* **2003**, *107*, 570.

(42) Smith, K.-T.; Tilset, M.; Kuhlman, R.; Caulton, K. G. *J. Am. Chem. Soc.* **1995**, *117*, 9473.

(43) Gusev, D. G.; Dolgushin, F. M.; Antipin, M. Y. *Organometallics* **2001**, *20*, 1001.

(44) Gross, C. L.; Girolami, G. S. *Organometallics* **2007**, *26*, 1658.

(45) Webster, C. E.; Gross, C. L.; Young, D. M.; Girolami, G. S.; Schultz, A. J.; Hall, M. B.; Eckert, J. *J. Am. Chem. Soc.* **2005**, *127*, 15091.

(46) Kubas, G. J. *Metal Dihydrogen and σ -Bond Complexes*; Kluwer Academic/Plenum Publishers: New York, 2001.

(47) Esteruelas, M. A.; Gómez, A. V.; Lahoz, F. J.; López, A. M.; Oñate, E.; Oro, L. A. *Organometallics* **1996**, *15*, 3423.

(48) Esteruelas, M. A.; Gómez, A. V.; López, A. M.; Oro, L. A. *Organometallics* **1996**, *15*, 878.

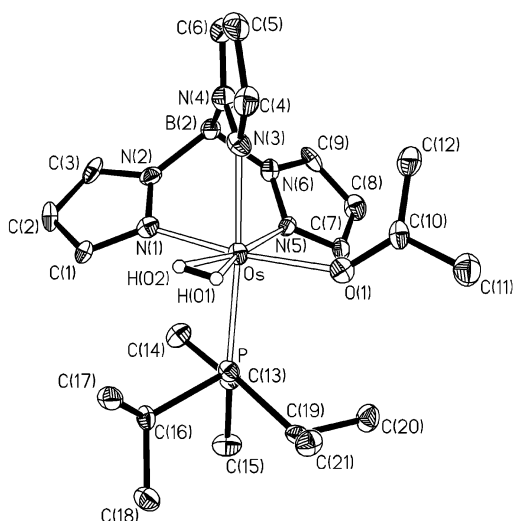


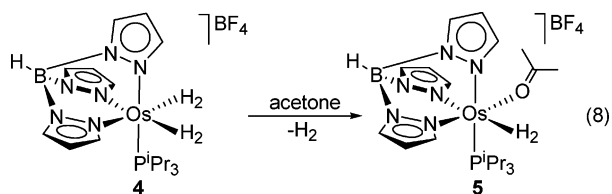
Figure 11. Molecular diagram of the cation of complex **5**. Selected bond lengths (Å) and angles (deg): Os–P 2.356(2), Os–O(1) 2.121(5), Os–N(1) 2.062(6), Os–N(3) 2.111(6), Os–N(5) 2.113(6), Os–H(01) 1.79(5), Os–H(02) 1.79(5), O(1)–C(10) 1.236(8), H(01)–H(02) 0.8(1); P–Os–O(1) 95.57(15), P–Os–N(1) 93.92(18), P–Os–N(3) 176.02(18), P–Os–N(5) 94.78(17), O(1)–Os–N(1) 172.8(2), O(1)–Os–N(3) 92.3(2), O(1)–Os–N(5) 87.2(2), O(1)–Os–H(01) 77(3), O(1)–Os–H(02) 101(3), N(1)–Os–N(3) 82.4(2), N(1)–Os–N(5) 87.7(2), N(1)–Os–H(01) 107(3), N(1)–Os–H(02) 83(3), N(3)–Os–H(01) 91(3), N(3)–Os–H(02) 87(3), N(3)–Os–N(5) 86.5(2), H(01)–Os–H(02) 24(3).

(dihydrogen) nature of **4**, since it is not reasonable that the size of the Tp and Cp can affect the coordination mode of the smallest known ligand.

3. Sequential Displacement of the Hydrogen Molecules.

A characteristic of the dihydrogen ligand is its high tendency to undergo dissociation from the metal center. In accordance with this, complex **4** releases the coordinated hydrogen molecules in a sequential manner. The resulting metallic fragments are stabilized by coordination of acetone.

At room temperature, the stirring of acetone solutions of **4** under a slight flow of argon for 3 h affords the dihydrogen-solvate compound $[\text{OsTp}(\eta^2\text{-H}_2)(\kappa^1\text{-OCMe}_2)(\text{P}^i\text{Pr}_3)]\text{BF}_4$ (**5**), which is isolated as a yellow solid in 78% yield, according to eq 8.



Complex **5** was also characterized by X-ray diffraction analysis. Figure 11 shows a view of the cation of this compound. The geometry around the osmium atom can be described as a distorted octahedron with the coordinating nitrogen atoms of the Tp ligand in *fac* sites. The metal coordination sphere is completed by the phosphine ligand *trans* disposed to N(3) (P–Os–N(3) = 176.02(18)°), the acetone molecule *trans* disposed to N(1) (O(1)–Os–N(1) = 172.8(2)°), and the dihydrogen ligand *trans* disposed to N(5). The Os–O(1) bond length of 2.121(5) Å agrees well with the osmium–oxygen distances found in other osmium–ketone compounds.^{9c,f,g,11,28,49} The B3LYP-optimized structure of the model complex $[\text{OsTp}(\eta^2\text{-H}_2)(\kappa^1\text{-OCMe}_2)(\text{PMe}_3)]^+$ (**5t**) supports the dihydrogen formulation (Figure 12). The H(01)–H(02) separation is 0.916 Å.

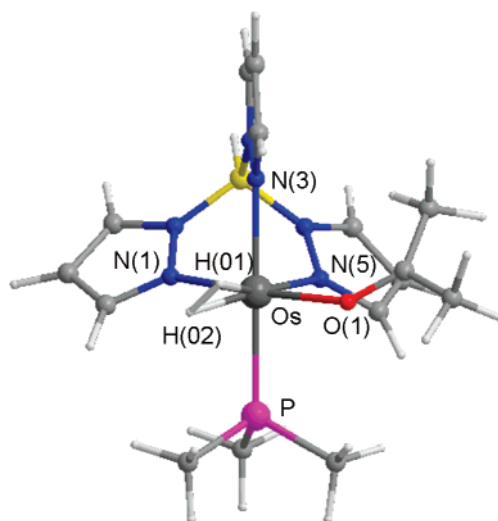


Figure 12. Optimized structure of the cation **5t**. Selected bond lengths (Å) and angles (deg): Os–H(01) 1.707, Os–H(02) 1.700, H(01)–H(02) 0.916; O(1)–Os–N(5) 91.3, O(1)–Os–H(01) 78.3, O(1)–Os–H(02) 101.7, N(1)–Os–N(5) 86.6, N(1)–Os–H(01) 103.1, N(1)–Os–H(02) 80.8, N(3)–Os–H(01) 81.8, N(3)–Os–H(02) 100.9, H(01)–Os–H(02) 31.2.

A weakening of the C–O double bond of the acetone ligand as a consequence of the coordination of the oxygen atom to the metal center is revealed by the IR of **5** in Nujol, which shows the $\nu(\text{CO})$ band at 1646 cm^{-1} , shifted 69 cm^{-1} to lower wavenumbers if compared with the free molecule (1715 cm^{-1}). The effect of the coordination is also evident in the $^{13}\text{C}\{^1\text{H}\}$ NMR spectrum, where the carbonyl resonance appears at 228.9 ppm, shifted 22.9 ppm to lower field with regard to the resonance of the free acetone (206 ppm).

In contrast to **3** and **4**, at room temperature the skeleton of **5** is rigid in solution. In accordance with this, at 298 K the ^1H NMR spectrum of **5** in acetone- d_6 shows three sets of pyrazolyl resonances between 8.37 and 6.33 ppm. In the high-field region of the spectrum, the dihydrogen ligand gives rise to a doublet ($J_{\text{H-P}} = 8.0$ Hz) at -5.62 ppm. For this resonance a $T_{1(\text{min})}$ value of 19 ± 1 ms was obtained at 208 K in the 300 MHz scale. Assuming fast spinning, this value corresponds to a hydrogen–hydrogen separation of 0.92 Å, which is the same as that obtained by DFT calculations.

The Cp counterpart of **5** is the dihydride $[\text{OsH}_2\text{Cp}(\kappa^1\text{-OCMe}_2)(\text{P}^i\text{Pr}_3)]\text{BF}_4$, which is prepared by the same procedure as **5**, starting from $[\text{OsH}_2\text{Cp}(\eta^2\text{-H}_2)(\text{P}^i\text{Pr}_3)]\text{BF}_4$ (Scheme 1). On the basis of the ^1H NMR spectrum and the X-ray structure of the related complex $[\text{OsH}_2\text{Cp}\{\kappa^1\text{-OC}(\text{CH}_3)\text{CH}=\text{CHPh}\}(\text{P}^i\text{Pr}_3)]\text{BAr}^{\text{F}_4}$,¹¹ a four-legged piano stool geometry with *transoid*-hydride ligands is proposed for this derivative.¹² This distribution of ligands around the osmium atom agrees well with the B3LYP-optimized structure (Figure 13a) of the model complex $[\text{OsH}_2\text{-Cp}(\kappa^1\text{-OCMe}_2)(\text{PMe}_3)]^+$ (*transoid*-**5t**_{Cp}). In addition, it should be mentioned that a *cisoid*-dihydride structure (Figure 13b) is also a minimum, which lies 3.2 $\text{kcal}\cdot\text{mol}^{-1}$ above *transoid*-**5t**_{Cp}. This small difference is not consistent with the experimental fact that complex $[\text{OsH}_2\text{Cp}(\kappa^1\text{-OCMe}_2)(\text{P}^i\text{Pr}_3)]\text{BF}_4$ has a rigid structure in solution at room temperature. Because in the *cisoid* isomer the acetone molecule is situated *cisoid* to the phosphine ligand (P–Os–O = 88.7°), one should expect that

(49) (a) Barrio, P.; Castarlenas, R.; Esteruelas, M. A.; Lledós, A.; Maseras, F.; Oñate, E.; Tomàs, J. *Organometallics* **2001**, *20*, 442. (b) Barrio, P.; Castarlenas, R.; Esteruelas, M. A.; Oñate, E. *Organometallics* **2001**, *20*, 2635.

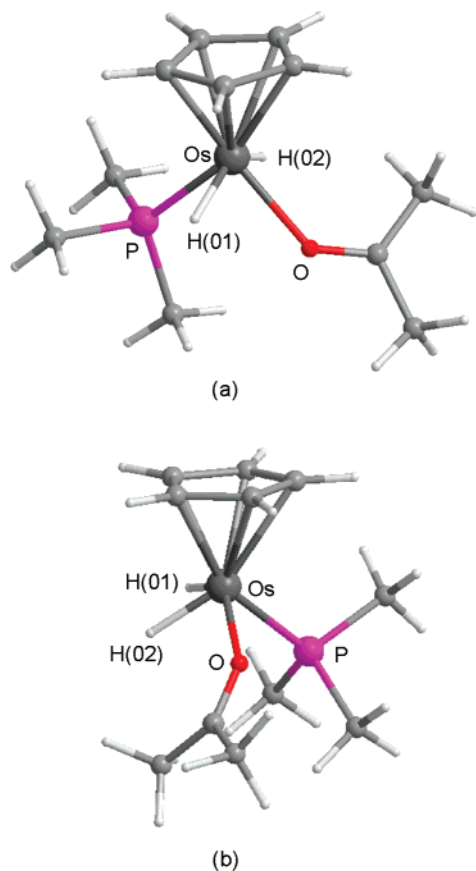


Figure 13. Optimized structures of the cations *transoid-5t_{Cp}* (a) and *cisoid-5t_{Cp}* (b). (a) Selected bond lengths (Å) and angles (deg): Os–H(01) 1.630, Os–H(02) 1.635; H(01)–Os–H(02) 134.7. (b) Selected bond lengths (Å) and angles (deg): Os–H(01) 1.599, Os–H(02) 1.610; H(01)–Os–H(02) 63.4.

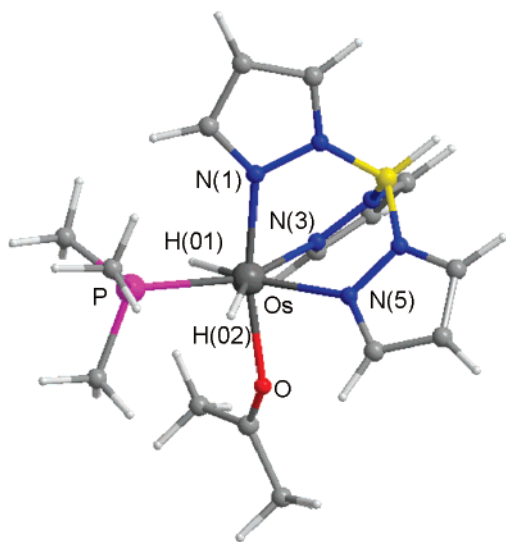


Figure 14. Optimized structure of the cation **5t₁**. Selected bond lengths (Å) and angles (deg): Os–H(01) 1.630, Os–H(02) 1.626; P–Os–H(01) 67.3, P–Os–H(02) 61.5, N(3)–Os–H(01) 77.1, N(3)–Os–N(5) 86.2, N(5)–Os–H(02) 73.8.

the replacement of the methyl groups by the real isopropyl substituents of the phosphine ligands produces the destabilization of the *cisoid*-dihydride structure.

Complex **5t** also has a dihydride isomer, [OsH₂Tp(κ¹-OCMe₂)(PMe₃)]⁺ (**5t₁**), which lies 11.3 kcal·mol^{−1} above **5t** (Figure 14). In contrast to **5t_{Cp}** but in agreement with **3** and **3t**,

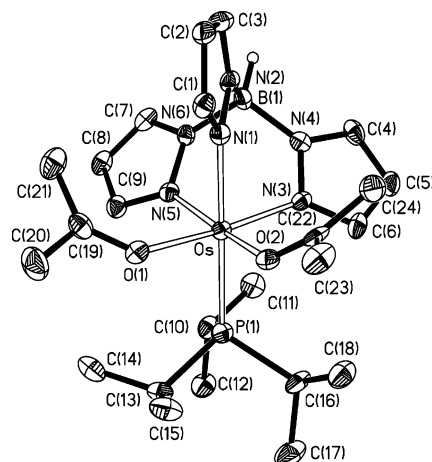


Figure 15. Molecular diagram of the cation of complex **6**. Selected bond lengths (Å) and angles (deg): Os–P(1) 2.3449(13), Os–O(1) 2.097(3), Os–O(2) 2.100(3), Os–N(1) 2.087(4), Os–N(3) 2.050(4), Os–N(5) 2.040(4), O(1)–C(19) 1.244(5), O(2)–C(22) 1.241(5); P(1)–Os–O(1) 93.10(9), P(1)–Os–O(2) 96.03(9), P(1)–Os–N(1) 179.62(11), P(1)–Os–N(3) 93.92(11), P(1)–Os–N(5) 93.78(11), O(1)–Os–N(1) 86.55(13), O(1)–Os–N(3) 172.34(13), O(1)–Os–N(5) 94.82(13), O(1)–Os–O(2) 76.87(12), O(2)–Os–N(1) 84.02(13), O(2)–Os–N(3) 99.31(13), O(2)–Os–N(5) 167.45(13), N(1)–Os–N(3) 86.45(14), N(1)–Os–N(5) 86.12(14), N(3)–Os–N(5) 87.79(14).

the structure of this species can be described as a pentagonal bipyramid. The acetone molecule lies in an axial position *trans* disposed to the N(1) nitrogen atom (O(1)–Os–N(1) = 169.2°), while the phosphine group is located in the equatorial plane between the hydride ligands (P–Os–H(01) = 67.3° and P–Os–H(02) = 61.5°). This structure is a new example showing how the Tp ligand enforces dispositions allowing N–Os–N close to 90°.

The differences between **5** and its Cp counterpart are not limited to the nature of the OsH₂ unit and their structures, but also involve the behavior of both compounds in solution. In contrast to [OsH₂Cp(κ¹-OCMe₂)(PⁱPr₃)]BF₄, which is stable, complex **5** in acetone at reflux loses molecular hydrogen overnight. The resulting metal fragment coordinates a second solvent molecule to give the bis-solvento compound [OsTp(κ¹-OCMe₂)₂(PⁱPr₃)]BF₄ (**6**), which is isolated as an orange solid in 62% yield (eq 9).

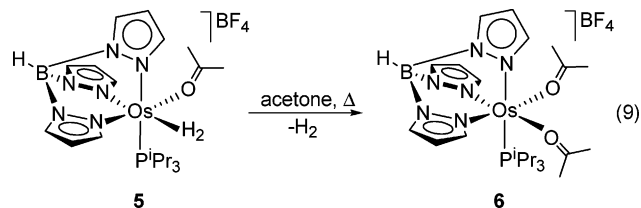


Figure 15 shows a view of the X-ray structure of the cation of **6**. The geometry around the osmium atom can be described as a distorted octahedron with the Tp ligand occupying *fac* positions, with N(1)–Os–P(1), N(3)–Os–O(1), and N(5)–Os–O(2) angles of 179.62(11)°, 172.34(13)°, and 167.45(13)°, respectively. The Os–O distances of 2.097(3) Å (Os–O(1)) and 2.100(3) Å (Os–O(2)) compare well with that of **5**.

The IR and ¹³C{¹H} and ¹H NMR spectra of **6** are consistent with the structure shown in Figure 15. In the IR spectrum the most noticeable feature is the presence of a ν(CO) band at 1640 cm^{−1}, corresponding to the coordinated acetone molecules. In the ¹³C{¹H} NMR spectrum, the carbonyl groups of these

equivalent ligands give rise to a singlet at 226.2 ppm. The ^1H NMR spectrum in acetone- d_6 at room temperature shows two sets of pyrazolyl resonances between 8.12 and 6.42 ppm, indicating that in solution the skeleton of **6** is rigid.

Concluding Remarks. This paper shows an entry to the chemistry of the $\text{OsTp}(\text{P}^i\text{Pr}_3)$ unit, which has afforded new hydride, dihydrogen, and acetone OsTp complexes, including a novel bis(dihydrogen) derivative. The starting point is the trihydride $\text{OsH}_3\text{Cl}(\text{P}^i\text{Pr}_3)_2$, which reacts with KTp to give $\text{OsH}_3\text{-Tp}(\text{P}^i\text{Pr}_3)$ via a $\kappa^2\text{-Tp}$ intermediate, isolated and characterized by X-ray diffraction analysis and DFT calculations. The protonation of $\text{OsH}_3\text{Tp}(\text{P}^i\text{Pr}_3)$ leads to $[\text{OsTp}(\eta^2\text{-H}_2)_2(\text{P}^i\text{Pr}_3)]\text{-BF}_4$. This compound not only is a rare example of bis(dihydrogen) species that does not contain any hydride co-ligand but is further the key to new findings. In acetone it releases molecular hydrogen in a sequential manner to afford the solvate derivatives $[\text{OsTp}(\eta^2\text{-H}_2)(\kappa^1\text{-OCMe}_2)(\text{P}^i\text{Pr}_3)]\text{BF}_4$ and $[\text{OsTp}(\kappa^1\text{-OCMe}_2)_2(\text{P}^i\text{Pr}_3)]\text{BF}_4$, which are allowing us to develop interesting novel OsTp chemistry with organic unsaturated substrates.⁵⁰

The structures of the new complexes and those of their Cp counterparts are also systematically compared. The study reveals that Tp avoids the piano stool structures, typical for the Cp ligand, and enforces dispositions allowing N–Os–N angles close to 90° such as pentagonal bipyramid and octahedron. These structures appear to favor the nonclassical interactions between the hydrogen atoms bonded to the metal center. As a consequence of this, the thermally activated site exchange processes of hydride ligands and the loss of molecular hydrogen are favored in the OsTp compounds with regard to the OsCp counterparts.

In conclusion, we have discovered an easy entry to the $\text{OsTp}(\text{P}^i\text{Pr}_3)$ unit, which allows approaching new targets in Os-hydride chemistry and to compare the $\text{OsTp}(\text{P}^i\text{Pr}_3)$ complexes with their $\text{OsCp}(\text{P}^i\text{Pr}_3)$ counterparts.

Experimental Section

General Methods and Instrumentation. All reactions were carried out under argon with rigorous exclusion of air using Schlenk-tube or glovebox techniques. Solvents were dried by the usual procedures and distilled under argon prior to use. The starting material $\text{OsH}_3\text{Cl}(\text{P}^i\text{Pr}_3)_2$ was prepared according to the published method.⁵¹ The following reagents were obtained from commercial sources: KTp (Alfa Aesar), $\text{HBF}_4\cdot\text{Et}_2\text{O}$ (Fluka), and NaBPh_4 (Sigma-Aldrich). CDFCl_2 was prepared by a reported procedure.⁵² ^1H , $^{31}\text{P}\{^1\text{H}\}$, and $^{13}\text{C}\{^1\text{H}\}$ NMR spectra were recorded on either a Varian Gemini 2000, a Bruker ARX 300, a Bruker Avance 300 MHz, or a Bruker Avance 400 MHz instrument. Chemical shifts (expressed in parts per million) are referenced to residual solvent peaks (^1H , $^{13}\text{C}\{^1\text{H}\}$) or external H_3PO_4 ($^{31}\text{P}\{^1\text{H}\}$). Coupling constants, J , are given in hertz. Integration ratios were measured with long repetition times (10 s) to avoid relaxation problems. Infrared spectra were run on a Perkin-Elmer 1730 spectrometer (Nujol mulls on polyethylene sheets). C, H, and N analyses were carried out in a Perkin-Elmer 2400 CHNS/O analyzer.

Preparation of $\text{Os}(\kappa^2\text{-Tp})\text{H}_3(\text{P}^i\text{Pr}_3)_2$ (2**).** THF (10 mL) was added to a mixture of $\text{OsH}_3\text{Cl}(\text{P}^i\text{Pr}_3)_2$ (**1**) (400 mg, 0.73 mmol) and KTp (294 mg, 1.17 mmol). The reacting suspension was stirred for 20 min at room temperature. The solvent was removed *in vacuo* and the foamy residue extracted with pentane (10 × 15 mL). The combined extracts were concentrated to ca. 5 mL and cooled to

–70 °C. A white solid precipitated, which was separated by decantation and dried *in vacuo*. Yield: 451 mg (85%). Anal. Calcd for $\text{C}_{27}\text{H}_{55}\text{BN}_6\text{OsP}_2$: C, 44.62; H, 7.63; N, 11.56. Found: C, 44.45; H, 7.88; N, 11.56. IR (Nujol, cm^{-1}): $\nu(\text{BH})$ 2450 (m), $\nu(\text{OsH})$ 2167 (m), 2125 (m). ^1H NMR (300 MHz, C_7D_8 , 298 K): 7.98 (d, 1H, Tp), 7.93 (d, 2H, Tp), 7.86 (d, 1H, Tp), 7.04 (d, 2H, Tp), 6.38 (t, 1H, Tp), 6.00 (t, 2H, Tp), 2.15 (m, 3H, PCH), 1.73 (m, 3H, PCH), 1.01 (dd, $J_{\text{H-P}} = 11.4$, $J_{\text{H-H}} = 7.2$, 18H, PCHCH_3), 0.95 (dd, $J_{\text{H-P}} = 10.8$, $J_{\text{H-H}} = 6.9$, 18H, PCHCH_3), –11.94 (t, $J_{\text{H-P}} = 12.6$, 3H, OsH), all coupling constants for the pyrazolyl proton resonances were about 2 Hz. $T_{1(\text{min})}$ (ms, OsH_3 , 300 MHz, C_7D_8): 70 ± 1 (238 K). $^{31}\text{P}\{^1\text{H}\}$ NMR (121.49 MHz, C_6D_6 , 298 K): 22.9 (AB spin system, $\Delta\nu = 412.2$, $J_{\text{A-B}} = 279$). $^{13}\text{C}\{^1\text{H}\}$ NMR (75.48 MHz, C_6D_6 , 298 K): 148.5 (s, Tp), 142.4 (s, Tp), 136.4 (s, Tp), 135.2 (s, Tp), 106.3 (s, Tp), 105.0 (s, Tp), 28.5 (dd, $J_{\text{C-P}} = 20$, $J_{\text{C-P}} = 4$, PCH), 23.2 (dd, $J_{\text{C-P}} = 19$, $J_{\text{C-P}} = 3$, PCH), 20.0 (s, PCHCH_3), 19.4 (s, PCHCH_3).

Preparation of $\text{OsTpH}_3(\text{P}^i\text{Pr}_3)$ (3**).** A solution of **2** (414 mg, 0.57 mmol) in 20 mL of toluene was heated at 80 °C for 7 h in a Schlenk flask equipped with a Teflon stopcock. After this time it was allowed to reach room temperature and then the solution was filtered through Celite and the toluene evaporated *in vacuo*. The residue was washed with pentane (5 × 3 mL) and vacuum-dried. A white solid was obtained. Yield: 226 mg (70%). Anal. Calcd for $\text{C}_{18}\text{H}_{34}\text{BN}_6\text{OsP}$: C, 38.16; H, 6.05; N, 14.83. Found: C, 38.03; H, 5.98; N, 14.50. IR (Nujol, cm^{-1}): $\nu(\text{BH})$ 2467 (m), $\nu(\text{OsH})$ 2130 (m), 2086 (m). ^1H NMR (400 MHz, C_7D_8 , 298 K): 7.82, 7.39, 5.83 (9H, 3:3:3 integration, all br, Tp), 1.92 (m, 3H, PCH), 1.04 (dd, $J_{\text{H-P}} = 12.3$, $J_{\text{H-H}} = 7.1$, 18H, PCHCH_3), –10.43 (d, $J_{\text{H-P}} = 15.0$, 3H, OsH). ^1H NMR (400 MHz, C_7D_8 , 243 K): 7.87 (d, 2H, Tp), 7.71 (br, 1H, Tp), 7.42 (d, 2H, Tp), 7.29 (d, 1H, Tp), 5.86 (t, 2H, Tp), 5.64 (t, 1H, Tp), 1.81 (m, 3H, PCH), 1.03 (dd, $J_{\text{H-P}} = 12.2$, $J_{\text{H-H}} = 7.0$, 18H, PCHCH_3), –10.10 (d, $J_{\text{H-P}} = 14.7$, 3H, OsH), all coupling constants for the pyrazolyl proton resonances were about 1.5 Hz. $T_{1(\text{min})}$ (ms, OsH_3 , 400 MHz, C_7D_8): 100 ± 1 (238 K). $^{31}\text{P}\{^1\text{H}\}$ NMR (121.49 MHz, C_6D_6 , 298 K): 28.7 (s). $^{13}\text{C}\{^1\text{H}\}$ NMR (75.48 MHz, C_6D_6 , 298 K): 146.2, 134.0, 105.6 (all br, Tp), 24.9 (d, $J_{\text{C-P}} = 26.0$, PCH), 20.2 (s, PCHCH_3). $^{13}\text{C}\{^1\text{H}\}$ NMR (100.62 MHz, C_7D_8 , 243 K): 147.2, 145.4, 134.2, 132.7, 129.1, 105.6 (all s, Tp), 23.9 (d, $J_{\text{C-P}} = 27$, PCH), 20.3 (s, PCHCH_3).

Preparation of $[\text{OsTp}(\eta^2\text{-H}_2)_2(\text{P}^i\text{Pr}_3)]\text{BF}_4$ (4**).** A solution of **3** (350 mg, 0.62 mmol) in 8 mL of diethyl ether was treated with $\text{HBF}_4\cdot\text{Et}_2\text{O}$ (101 μL , 0.74 mmol). Immediately a white solid appeared. The solid was separated by decantation, washed with diethyl ether (3 × 5 mL), and dried *in vacuo*. Yield: 370 mg (91%). Anal. Calcd for $\text{C}_{18}\text{H}_{35}\text{B}_2\text{F}_4\text{N}_6\text{OsP}$: C, 33.04; H, 5.39; N, 12.84. Found: C, 33.21; H, 5.35; N, 12.87. IR (Nujol, cm^{-1}): $\nu(\text{BH})$ 2497 (s), $\nu(\text{BF}_4)$ 1047 (br, s). ^1H NMR (300 MHz, CD_2Cl_2 , 298 K): 7.95 (d, 3H, Tp), 7.76 (d, 3H, Tp), 6.34 (t, 3H, Tp), 2.48 (m, 3H, PCH), 1.12 (dd, $J_{\text{H-P}} = 14.1$, $J_{\text{H-H}} = 7.1$, 18H, PCHCH_3), –8.51 (d, $J_{\text{H-P}} = 7.5$, 4H, OsH), all coupling constants for the pyrazolyl proton resonances were about 2 Hz. ^1H NMR (300 MHz, CD_2Cl_2 , 193 K): 8.11 (s, 1H, Tp), 7.78 (s, 4H, Tp), 7.65 (s, 1H, Tp), 6.32 (s, 2H, Tp), 6.23 (s, 1H, Tp), 2.35 (br, 3H, PCH), 0.90 (m, 18H, PCHCH_3), –8.60 (br, 4H, OsH). $T_{1(\text{min})}$ (ms, $\text{Os}(\text{H}_2)_2$, 300 MHz, CD_2Cl_2): 12 ± 1 (208 K). $^{31}\text{P}\{^1\text{H}\}$ NMR (121.49 MHz, CD_2Cl_2 , 298 K): 20.1 (s). $^{13}\text{C}\{^1\text{H}\}$ NMR (75.48 MHz, CD_2Cl_2 , 298 K): 147.9, 136.9, 108.0 (all br, Tp), 23.7 (d, $J_{\text{C-P}} = 30$, PCH), 19.4 (s, PCHCH_3). $^{13}\text{C}\{^1\text{H}\}$ NMR (75.48 MHz, CD_2Cl_2 , 193 K): 147.0, 146.1, 136.5, 135.0, 107.2, 106.6 (all s, Tp), 21.9 (br, PCH), 18.5, 16.3 (br, PCHCH_3).

Preparation of $[\text{OsTp}(\eta^2\text{-H}_2)(\kappa^1\text{-OCMe}_2)(\text{P}^i\text{Pr}_3)]\text{BF}_4$ (5**).** **4** (416 mg, 0.73 mmol) was dissolved in 10 mL of acetone and stirred for 3 h at room temperature under a flow of argon. The resulting yellow solution was concentrated to ca. 1 mL. The addition of diethyl ether (7 mL) caused the precipitation of a yellow solid,

(50) Castro-Rodrigo, R. Ph.D. Dissertation, University of Zaragoza, 2006–2010.

(51) Gusev, D. G.; Kuhlman, R.; Sini, G.; Eisenstein, O.; Caulton, K. G. *J. Am. Chem. Soc.* **1994**, *116*, 2685.

(52) Siegel, J.; Anet, F. A. L. *J. Org. Chem.* **1988**, *53*, 2629.

Table 1. Crystal Data and Data Collection and Refinement for 2, 3, 4, 5, and 6

	2	3	4	5	6
Crystal Data					
formula	C ₂₇ H ₅₅ BN ₆ OsP ₂	C ₁₈ H ₃₄ BN ₆ OsP	C ₁₈ H ₃₅ B ₂ F ₄ N ₆ OsP	C ₂₁ H ₃₉ B ₂ F ₄ N ₆ OOSp	C ₄₈ H ₆₃ B ₂ N ₆ O ₂ OsP
molecular wt	726.72	566.49	654.31	710.37	998.83
color and habit	colorless, prism	colorless, prism	colorless, irregular block	yellow, irregular block	orange, irregular block
size, mm	0.10, 0.10, 0.08	0.10, 0.16, 0.04	0.08, 0.04, 0.02	0.16, 0.06, 0.02	0.10, 0.10, 0.08
symmetry, space group	monoclinic, <i>P</i> 2(1)/ <i>n</i>	monoclinic, <i>P</i> 2(1)/ <i>n</i>	triclinic, <i>P</i> $\bar{1}$	monoclinic, <i>P</i> 2(1)/ <i>c</i>	monoclinic, <i>P</i> 2(1)/ <i>n</i>
<i>a</i> , Å	12.480(3)	11.1756(15)	12.094(8)	10.6370(12)	12.7118(14)
<i>b</i> , Å	17.862(5)	14.3048(19)	14.667(10)	16.6865(19)	19.539(2)
<i>c</i> , Å	14.570(4)	14.1995(18)	15.333(10)	15.5819(18)	18.658(2)
α , deg			112.807(13)		
β , deg	94.947(5)	107.577(2)	100.268(16)	94.240(2)	91.351(2)
γ , deg			92.698(13)		
<i>V</i> , Å ³	3235.9(15)	2164.0(5)	2447(3)	2758.1(5)	4632.9(9)
<i>Z</i>	4	4	4	4	4
<i>D</i> _{calc} , g cm ⁻³	1.492	1.739	1.776	1.711	1.432
Data Collection and Refinement					
diffractometer	Bruker Smart APEX				
λ (Mo K α), Å	0.71073				
monochromator	graphite oriented				
scan type	ω scans				
μ , mm ⁻¹	4.066	5.982	5.326	4.734	2.832
2 θ , range deg	3, 57	4, 58	3, 57	4, 57	4, 58
temp, K	100.0(2)	100.0(2)	100.0(2)	100.0(2)	100.0(2)
no. of data collected	40 006	26 930	30 713	32 091	57 954
no. of unique data	8015 (<i>R</i> _{int} = 0.0640)	5428 (<i>R</i> _{int} = 0.0621)	11 724 (<i>R</i> _{int} = 0.1227)	6712 (<i>R</i> _{int} = 0.0991)	11 535 (<i>R</i> _{int} = 0.0982)
no. of params/restraints	356/13	265/3	620/28	344/2	554/0
<i>R</i> ₁ ^a [<i>F</i> ² > 2 σ (<i>F</i> ²)]	0.0362	0.0302	0.0535	0.0620	0.0447
<i>wR</i> ₂ ^b [all data]	0.0748	0.0458	0.0907	0.1150	0.0784
<i>S</i> ^c [all data]	0.905	0.827	0.745	1.166	0.828

^a $R_1(F) = \sum ||F_o| - |F_c|| / \sum |F_o|$. ^b $wR_2(F^2) = \{ \sum [w(F_o^2 - F_c^2)^2] / \sum [w(F_o^2)^2] \}^{1/2}$. ^c $\text{Goof} = S = \{ \sum [F_o^2 - F_c^2]^2 / (n - p) \}^{1/2}$, where *n* is the number of reflections and *p* is the number of refined parameters.

which was separated by decantation, washed with diethyl ether (2 × 5 mL), and vacuum-dried. Yield: 407 mg (78%). Anal. Calcd for C₂₁H₃₉B₂F₄N₆OOSp: C, 35.50; H, 5.53; N, 11.83. Found: C, 35.34; H, 5.92; N, 11.61. IR (Nujol, cm⁻¹): ν (BH) 2492 (m), ν (CO) 1646 (s), ν (BF₄) = 1057 (br, s). ¹H NMR (300 MHz, (CD₃)₂CO, 298 K): 8.37 (d, 1H, Tp), 8.28 (d, 1H, Tp), 7.98 (d, 2H, Tp), 7.93 (d, 1H, Tp), 7.77 (d, 1H, Tp), 6.64 (t, 1H, Tp), 6.39 (t, 1H, Tp), 6.33 (t, 1H, Tp), 2.66 (m, 3H, PCH), 2.21 (s, 6H, CH₃), 1.30 (dd, *J*_{H-P} = 13.7, *J*_{H-H} = 7.4, 9H, PCHCH₃), 1.23 (dd, *J*_{H-P} = 13.1, *J*_{H-H} = 7.4, 9H, PCHCH₃), -5.62 (d, *J*_{H-P} = 8.0, 1H, OsH), all coupling constants for the pyrazolyl proton resonances were about 2 Hz. *T*_{1(min)} (ms, 300 MHz, (CD₃)₂CO): 19 ± 1 (208 K). ³¹P{¹H} NMR (121.49 MHz, (CD₃)₂CO, 298 K): 6.8 (s). ¹³C{¹H} NMR (75.48 MHz, (CD₃)₂CO, 298 K): 228.9 (s, CO), 152.3, 147.3, 146.6, 139.6, 138.8, 137.3, 109.3, 109.1, 108.4 (all s, Tp), 31.6 (s, CH₃), 25.8 (d, *J*_{C-P} = 28, PCH), 21.0 (s, PCHCH₃).

Preparation of [OsTp(κ^1 -OCMe₂)₂(PⁱPr₃)]BF₄ (6). A solution of **5** (200 mg, 0.28 mmol) in 10 mL of acetone was heated under reflux overnight. The resulting orange solution was concentrated to ca. 1 mL, and diethyl ether (10 mL) was added, causing the formation of an orange solid, which was separated by decantation, washed with diethyl ether (2 × 7 mL), and dried *in vacuo*. Yield: 131 mg (62%). Anal. Calcd for C₂₂H₄₃B₂F₄N₆O₂OsP: C, 37.61; H, 5.65; N, 10.96. Found: C, 37.39; H, 5.77; N, 11.12. IR (Nujol, cm⁻¹): ν (BH) 2525 (w), ν (CO) 1640 (m), ν (BF₄) = 1049 (br, s). ¹H NMR (300 MHz, (CD₃)₂CO, 298 K): 8.12 (s, 1H, Tp), 8.06 (d, 2H, Tp), 7.91 (d, 2H, Tp), 7.38 (d, 1H, Tp), 6.49 (t, 1H, Tp), 6.42 (t, 1H, Tp), 2.80 (m, 3H, PCH), 2.21 (s, 12H, CH₃), 1.28 (dd, *J*_{H-P} = 12.5, *J*_{H-H} = 7.1, 18H, PCHCH₃), all coupling constants for the pyrazolyl proton resonances were about 2 Hz. ³¹P{¹H} NMR (121.49 MHz, (CD₃)₂CO, 298 K): -4.3 (s). ¹³C{¹H} NMR (75.48 MHz, (CD₃)₂CO, 298 K): 226.2 (s, CO), 151.4 (s, Tp), 142.3 (d,

*J*_{C-P} = 2, Tp), 139.1 (s, Tp), 137.4 (s, Tp), 108.6 (d, *J*_{P-C} = 3, Tp), 108.5 (s, Tp), 26.0 (d, *J*_{C-P} = 25, PCH), 20.6 (s, PCHCH₃).

Preparation of BPh₄ Salt of 6. An orange solution of **6** (50 mg, 0.07 mmol) in 7 mL of acetone was treated with NaBPh₄ (41 mg, 0.12 mmol). After 2 h, the solution was concentrated to ca. 1.5 mL and 20 mL of dichloromethane was added. The resulting suspension was filtered through Celite and the solvent removed by evaporation. The addition of 2 mL of acetone and 8 mL of diethyl ether caused the precipitation of an orange solid, which was separated by decantation and dried *in vacuo*. Yield: 35 mg (54%). The ³¹P and ¹H NMR data were identical to those reported for **6** except the additional ¹H signals of BPh₄⁻.

Fluxionality. The activation parameters for the exchange of axial and equatorial pyrazolyl ligands in **3** and **4** were determined by monitoring the ¹H NMR resonances of Tp ligands as a function of temperature. Complete line-shape analysis of the H⁴-pz region of these compounds was achieved using the program gNMR (Cherwell Scientific Publishing Limited). The rate constants for various temperatures were obtained by fitting calculated to experimental spectra by full line-shape iterations. The transverse relaxation time, *T*₂, was estimated at the lowest temperature. The activation parameters ΔH^\ddagger and ΔS^\ddagger were obtained by least-squares fit of $\ln(k/T)$ versus $1/T$ (Eyring equation). Error analysis assumed a 10% error in the rate constant and 1 K in the temperature. Errors were computed by published methods.⁵³

Structural Analysis of Complexes 2, 3, 4, 5, and 6. Crystals suitable for the X-ray diffraction study were obtained in pentane (**2** and **3**) or by slow diffusion of diethyl ether into concentrated solutions of the complexes in dichloromethane (**4**) or acetone (**5**

(53) Morse, P. M.; Spencer, M. D.; Wilson, S. R.; Girolami, G. S. *Organometallics* **1994**, *13*, 1646.

and the BPh₄ salt of **6**) at -20 °C. X-ray data were collected for all complexes on a Bruker Smart APEX CCD diffractometer equipped with a normal focus, 2.4 kW sealed tube source (Mo radiation, $\lambda = 0.71073$ Å) operating at 50 kV and 30 mA (**2**, **3**, **5**, **6**) or 40 mA (**4**). Data were collected over the complete sphere by a combination of four sets. Each frame exposure time was 10 s covering 0.3° in ω . Data were corrected for absorption by using a multiscan method applied with the SADABS program.⁵⁴ The structures of all compounds were solved by the Patterson method. Refinement, by full-matrix least-squares on F^2 with SHELXL97,⁵⁵ was similar for all complexes, including isotropic and subsequently anisotropic displacement parameters. The hydrogen atoms were observed or calculated and refined freely or using a restricted riding model. Hydride ligands were observed in the difference Fourier

(54) Blessing, R. H. *Acta Crystallogr.* **1995**, *A51*, 33. *SADABS*: Area-detector absorption correction; Bruker-AXS: Madison, WI, 1996.

(55) *SHELXTL* Package v. 6.10; Bruker-AXS: Madison, WI, 2000. Sheldrick, G. M. *SHELXS-86* and *SHELXL-97*; University of Göttingen: Göttingen, Germany, 1997.

(56) Frisch, M. J.; Trucks, G. W.; Schlegel, H. B.; Scuseria, G. E.; Robb, M. A.; Cheeseman, J. R.; Montgomery, J. A., Jr.; Vreven, T.; Kudin, K. N.; Burant, J. C.; Millam, J. M.; Iyengar, S. S.; Tomasi, J.; Barone, V.; Mennucci, B.; Cossi, M.; Scalmani, G.; Rega, N.; Petersson, G. A.; Nakatsuji, H.; Hada, M.; Ehara, M.; Toyota, K.; Fukuda, R.; Hasegawa, J.; Ishida, M.; Nakajima, T.; Honda, Y.; Kitao, O.; Nakai, H.; Klene, M.; Li, X.; Knox, J. E.; Hratchian, H. P.; Cross, J. B.; Adamo, C.; Jaramillo, J.; Gomperts, R.; Stratmann, R. E.; Yazyev, O.; Austin, A. J.; Cammi, R.; Pomelli, C.; Ochterski, J. W.; Ayala, P. Y.; Morokuma, K.; Voth, G. A.; Salvador, P.; Dannenberg, J. J.; Zakrzewski, V. G.; Dapprich, S.; Daniels, A. D.; Strain, M. C.; Farkas, O.; Malick, D. K.; Rabuck, A. D.; Raghavachari, K.; Foresman, J. B.; Ortiz, J. V.; Cui, Q.; Baboul, A. G.; Clifford, S.; Cioslowski, J.; Stefanov, B. B.; Liu, G.; Liashenko, A.; Piskorz, P.; Komaromi, I.; Martin, R. L.; Fox, D. J.; Keith, T.; Al-Laham, M. A.; Peng, C. Y.; Nanayakkara, A.; Challacombe, M.; Gill, P. M. W.; Johnson, B.; Chen, W.; Wong, M. W.; Gonzalez, C.; Pople, J. A. *Gaussian 03*, Revision C.02; Gaussian, Inc.: Wallingford, CT, 2004.

maps and refined as free isotropic atoms (**5**) or with restrained Os-H bond length (**2**, **3**, and **4**, 1.59(1) Å, CSD). Four methyl groups (C11, C12, C17, and C18) of one of the triisopropylphosphine ligands of complex **2** were refined in two positions (0.5). These groups were refined with an isotropic model and restrained geometry. For complex **4**, one of the two BF₄ anions was observed disordered. The anion was defined with two moieties, complementary occupancy factors, isotropic atoms, and restrained geometry. In all complexes, all the highest electronic residuals were observed in close proximity of the Os centers and make no chemical sense. Crystal data and details of the data collection and refinement are given in Table 1.

Computational Details. The calculations have been carried out using the Gaussian 03 computational package.⁵⁶ All the structures have been optimized using DFT and the B3LYP functional. The 6-31G** basis set has been used for all atoms but the Os, where the LANL2DZ basis and pseudopotential have been used instead. The transition states found have been confirmed by frequency calculations, and the connection between the starting and final reactants has been checked by slightly perturbing the TS geometry toward the minima geometries and reoptimizing.

Acknowledgment. Financial support from the MEC of Spain (Projects CTQ2005-00656 and Consolider Ingenio 2010 CSD2007-00006) and Diputación General de Aragón (E35) is acknowledged.

Supporting Information Available: X-ray analysis and crystal structure determinations, including bond lengths and angles of compounds **2**, **3**, **4**, **5**, and **6**. Orthogonal coordinates of the optimized theoretical structures. This material is available free of charge via the Internet at <http://pubs.acs.org>.

OM700480T